STUK

S T U K - **Y T O -** T R 1 8 1   August 2001

SPENT VVER FUEL CHARACTERISATION COMBINING A FORK DETECTOR WITH GAMMA SPECTROMETRY

Interim report on Task JNT A 1071 FIN of the Finnish Support Programme to IAEA Safeguards

A. Tiitta, J. Hautamäki
VTT Chemical Technology

In STUK this study was supervised by **Matti Tarvainen**

S T U K • S Ä T E I L Y T U R V A K E S K U S • S T R Å L S Ä K E R H E T S C E N T R A L E N
R A D I A T I O N   A N D   N U C L E A R   S A F E T Y   A U T H O R I T Y

The conclusions presented in the STUK report series are those of the authors
and do not necessarily represent the official position of STUK.

ABSTRACT

According to the IAEA's criteria a partial defect verification of spent fuel assemblies has to be performed before they become difficult to access. A partial defect test for spent fuel should be able to detect if half or more of the fuel pins have been removed from an assembly or possibly replaced by dummies. Therefore a partial defect test procedure needs to be developed by evolving the measurement systems and the analysis methods of the measurement data.

18 VVER assemblies were measured with an enhanced fork detector at the Loviisa KPA Store in May 2000. This measurement campaign is a follow-on to the campaigns conducted in 1999 at the Olkiluoto KPA Store, where BWR assemblies were measured using the same instrument.

The validity of correction methods developed in data analysis of Olkiluoto measurements was investigated in the analysis of Loviisa measurements. The share of ^{244}Cm neutron source out of the total neutron counts is derived from the results calculated with the PYVO code. The enrichment correction method to the neutron data corresponding to that used for BWR assemblies was applied for VVER assemblies. The contribution of other gamma emitting nuclides than ^{137}Cs was eliminated from the gross gamma signal with the help of gamma spectroscopy using the method developed for the BWR data. All these corrections were found to improve the essential correlations.

An assembly may have off-reactor cycles between irradiation cycles. The measured ^{137}Cs gamma signal can be corrected for off cycles using the recipes introduced in this report. Also the effect of off cycles to the neutron signal is contemplated. The correction for off cycles may be very important for a correct burnup verification of those assemblies, which have not been irradiated in sequential cycles.

CONTENTS

1 INTRODUCTION

The IAEA has to verify the LWR spent fuel assemblies at partial defect level before they become difficult to access. According to the IAEA's criteria a partial defect test for spent fuel should be able to detect if half or more of the fuel pins have been removed from an assembly or possibly replaced by dummies.

Capability of an enhanced fork detector for partial defect verification purposes by complementing the measurement results with theoretical calculations has been studied under Task JNT A 1071 FIN "Partial Defect Test on Spent Fuel LWRs". BWR assemblies were measured with the enhanced fork detector in the KPA Store in Olkiluoto in 1999. The data of these measurements have been analysed and reported earlier. [1] To perform the corresponding investigation for VVER-440 assemblies and to compare the analysis results of BWR and VVER assemblies a measurement campaign was conducted under this task in the KPA Store of the Loviisa NPP.

In an enhanced fork detector the total neutron count and the gross gamma measurements are complemented with a gamma-spectroscopic measurement using an integrated measurement head where a cadmium-zinc-telluride detector and a collimator are added to a conventional fork measurement head. The measurement system is described in reference [1].

The analysis methods, which were developed for Olkiluoto measurements, were applied also in Loviisa measurements. The share of ^{244}Cm neutron source out of the total neutron counts is calculated with the PYVO code. The neutron data are corrected for initial enrichment variation of the measured assemblies. The contribution of the main parasitic gamma emitting nuclides, i.e. ^{134}Cs and ^{106}Ru/Rh, is eliminated from the gross gamma signal with the help of gamma spectroscopy. [1]

The physical background of the hypothesis, that forms the basis of the idea of using a fork detector for partial defect verification, is discussed in section 2. The measurements are described in section 3. The data are analysed in section 4. The axial scanning measurements are presented in section 5. In section 6 conclusions are drawn based on the analysis of the measurement results.

2 PHYSICAL BACKGROUND

Burning nuclear fuel in a reactor produces both fission products and transuranium elements. The activity of a short-lived fission product nuclide eventually reaches saturation between its production rate and its decay, whereas the inventory of a long half-life nuclide tends to increase proportionally to the burnup. Here the half-life is compared to the total length of the irradiation period, typically 3-5 years. Some of the gamma-emitting nuclides are primary fission products and others are secondary products produced by a chain of neutron captures and beta decays from the primary products. This makes the picture about the correlation of different fission products and the irradiation history of the fuel somewhat more complicated in practice. [2]

A good candidate for a burnup indicator is ^{137}Cs with the half-life of 30.5 years. It could be expected that after a cooling time of more than twice the irradiation period ^{137}Cs would be the principal gamma-emitting activity. The relationship between the ^{137}Cs and the burnup is very linear.

Some of the transuranium isotopes produced during irradiation in the reactor emit neutrons through spontaneous fission. A long half-life spontaneously fissionable nuclide could also be used as a burnup indicator. The principal neutron emitter in the above mentioned cooling-time scale is ^{244}Cm with the half-life of 18.1 years. Due to formation of ^{244}Cm through several successive neutron captures of the parent nuclide ^{238}U, the relationship between the ^{244}Cm activity and the burnup is not linear, but can be described as a power function of burnup, with the power value typically 4…5. The value of the power may be dependent on the reactor and fuel type. [3] Combining the above mentioned two relationships leads to a relationship between the ^{137}Cs activity and the neutron yield originating from spontaneous fission of ^{244}Cm

$$N = k * A_{37}{}^{b} .\qquad (1)$$

Here N denotes the neutron yield from spontaneous fission of ^{244}Cm, A_{37} denotes the ^{137}Cs activity and b stands for the above-mentioned power.

The idea of using a fork detector for partial defect verification stems from a hypothesis that neutrons and gamma rays give a different view of a spent fuel assembly. Neutrons are highly penetrating in the medium giving signal over the whole volume of the fuel assembly whereas the strong self-absorption of gamma rays in uranium oxide fuel leads that the gamma rays detected outside the fuel assembly emanate predominantly from the surface of the fuel assembly. Therefore, the coefficient k in equation (1) should depend on the volume-to-surface ratio of the fuel assembly. This ratio reflects the geometrical configuration of the assembly. A partial defect, i.e. removal of fuel rods out of the assembly affects this ratio. E.g. removal of all internal rods of an 8*8–1 BWR assembly would reduce the volume density of fuel by 55 % leaving the apparent outer surface of the assembly untouched. This kind of defect is expected to give a measurement result, which significantly deviates from the correlation curve of non-defected assemblies of the same type given in equation (1). If this deviation exceeds the so-called error corridor of a single measurement around the correlation curve of equation (1), a partial defect is detected. The error corridor is defined by the total variation of a measurement result combining both the random effects attributed to the measurement itself and the real variation in the characteristics of the fuel assembly due to uncontrolled factors during its irradiation.

Recent availability of small room temperature operated CdZnTe detectors has opened a possibility to integrate gamma spectrometry into underwater devices such as a fork detector. One of the goals of this task is to find out the best experimental burnup indicator in connection with the partial defect verification.

3 MEASUREMENTS

3.1 Fuel data

The number of measured assemblies was 18. They are listed in Table I.

3.2 Measurements

The assemblies to be measured were brought from the storage pond to the evacuation pond by the fuel-handling machine. The accurate positioning of the fuel assembly between the prongs of the fork was made with the fuel handling machine, and the detector head was kept in a fixed position.

The total neutron counts, the gross gamma signal and the gamma spectrum of all assemblies listed in Table I were measured at three different heights, at 750, 1250 and 1750 mm from the lower end of the assemblies. The assemblies were measured at two azimuthal angles of 120° separation to even up possible azimuthal asymmetry.

Table I. Measured assemblies. The assemblies of type TBC are so-called fuel followers, which follow a control rod during irradiation. The type code PK denotes common assemblies.

Assembly ID	Type	IE (%)	Burnup (MWd/kg)	Date of evacuation from reactor	CT (days) as of 15.5.2000	Number of reactor cycles	Number of off-reactor cycles	Control cycles
13648120	PK	3.6	5.72	28.1.1995	1934	1 (9409–9501)		
22414764	TBC	2.4	22.39	18.8.1990	3558	2		
22424618	TBC	2.4	23.85	18.8.1990	3558	2		1. cycle
22432018	TBC	2.4	25.58	29.7.1995	1752	2		all cycles
13642705	PK	3.6	26.641	19.8.1995	1731	2		
22432046	TBC	2.4	27.72	12.9.1992	2802	2		all cycles
22421319	TBC	2.4	29.34	12.9.1992	2802	3 (8707–8908 and 9109–9210)	2	1. cycle
13617628	PK	3.6	30.63	8.7.1989	3964	3		
22432037	TBC	2.4	31.05	12.9.1992	2802	3		1. and 2. cycle
13632932	PK	3.6	32.86	4.9.1993	2445	3		
13640621	PK	3.6	34.68	19.8.1995	1731	3		
23632974	TBC	3.6	37.43	30.7.1994	2116	3		
23644402	TBC	3.6	39.11	16.8.1997	1003	3		2. cycle
13632903	PK	3.6	40.44	4.9.1993	2445	3		
13624637	PK	3.6	43.67	18.8.1990	3558	3		
13624432	PK	3.6	34.19	21.9.1996	1332	3 (8807–9008 and 9511–9609)	5	
13624532	PK	3.6	35.55	4.9.1993	2445	3 (8908–9009 and 9109–9309)	1	
13632649	PK	3.6	32.84	9.7.1994	2137	3 (9008–9209 and 9308–9407)	1	

Table II. *Coordinates of the axial scanning.*

z (mm)
2500
2250
2000
1750
1500
1250
1000
750
500
250
0

The assembly #13640621 was scanned axially at eleven vertical positions, see Table II.

The horizontal coordinates were kept constant in all measurements. The measurement arrangement is shown in Figure 1.
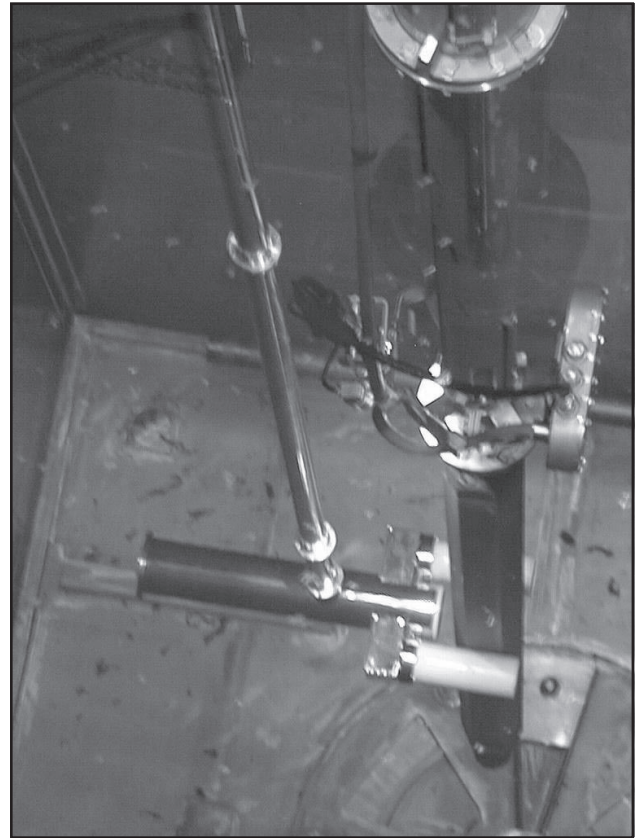
Figure 1. *An assembly in measurement position.*

4 DATA ANALYSIS

In this section first the measurements performed at the vertical level close to the mid-point of the assemblies (z = 1250 mm) are analysed. In section 4.3 the sensitivity to the vertical positioning is considered by analysing a series of measurements taken within one metre in the central region of the assembly.

All measured data points have been taken into consideration in the following fits. The measured raw data is given in Table A1.I in Annex 1.

The measurement data from two azimuthal angles have been averaged in the analysis described in sections 4.1, 4.2 and 4.3. The importance of the averaging the measurement data is contemplated in section 4.5.

4.1 Gamma measurements

4.1.1 Corrections applied to gamma signals

The cooling time of the measured assemblies varied from 2.7 to 11 years. The measured gamma spectrum of the youngest assembly #23644402 is shown in Figure 2.

The isotopes visible in the gross gamma signal are ^{137}Cs, ^{134}Cs, ^{154}Eu and ^{106}Ru/Rh. The contribution of ^{134}Cs and ^{106}Rh activities was eliminated from the gross gamma data and the gamma emission energy rate of ^{137}Cs (G_{37}) was calculated according to the following equation:

$$G_{37} = \frac{G}{1 + 2.620 * R_{34} + 0.324 * R_{06}}, \qquad (2)$$

where R_{34} stands for the measured activity ratio of ^{134}Cs to ^{137}Cs and R_{06} stands for the measured activity ratio of ^{106}Ru/Rh to ^{137}Cs obtained from the gamma spectrometric data. The activity ratios refer to the date when the measurements have been performed. The constants 2.620 and 0.324 have been calculated from the emissivities and energies of the gamma peaks. G denotes the measured and averaged gross gamma signal, which can be corrected for the cooling time of ^{137}Cs. In the remainder of this report the gross gamma denotes the
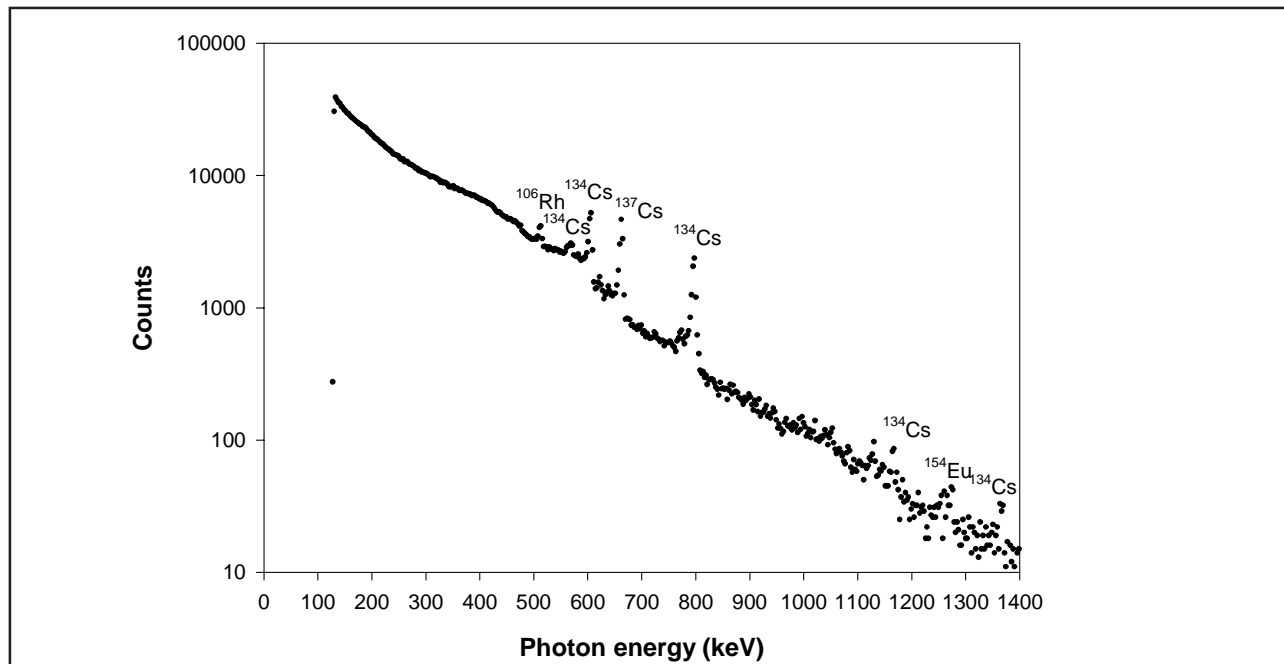

Figure 2. *Gamma spectrum of the youngest assembly #23644402, whose cooling time is about 2.7 years and burnup 39 MWd/kg.*

Table III. Parameters of the ^{137}Cs ratio vs. the ratio of irradiation years after off-cycles to the total number of irradiation cycles fits with different numbers of off-cycles.

Off cycles	p	σ_p	q	σ_q	R^2
1	0.9757	0.0001	0.0243	0.0001	1.0000
2	0.9547	0.0001	0.0453	0.0002	1.0000
3	0.9332	0.0005	0.0671	0.0007	0.9999
4	0.9112	0.0006	0.0891	0.0008	0.9999
5	0.8880	0.0003	0.1123	0.0004	0.9998

gross gamma signal corrected for ^{134}Cs and ^{106}Ru/Rh, whenever these isotopes contributed to gross gamma signal. The method has been described more in detail in ref. [1]. A very weak ^{154}Eu peak of 1274 keV was identified in many spectra. ^{154}Eu has not been taken into consideration in the gross gamma correction because the efficiency of the 20 mm^3 CZT detector did not permit accurate enough evaluation of the ^{154}Eu activity, which has the dominant peaks at high energies. The second strongest 723 keV peak of ^{154}Eu falls under the strong 796 keV peak of ^{134}Cs making it impossible to use that peak for ^{154}Eu analysis. For being able to use this peak a considerable improvement in the CZT detector resolution should be achieved. On the other hand a larger CZT detector, e.g. a 500 mm^3 one, could improve the high-energy efficiency of the gamma spectrometry, which might allow the use of 1274 keV peak of ^{154}Eu. This would imply changes in the gamma collimator and shielding, which might make the device construction impracticable. Anyway, the correction for ^{154}Eu is the next in importance and it should improve the quality of the corrected gross gamma data. Due to a considerably shorter half-life of ^{154}Eu as compared to ^{137}Cs the importance of ^{154}Eu decreases with increasing cooling time.

The current of the ionisation chambers is proportional to the absorbed dose rate. This indicates that the mass energy-absorption coefficient for different gamma energies should be taken into consideration in equation (2). The mass energy-absorption coefficient varies from 0.0287–0.0279 in energy interval 0.3 MeV–1 MeV in nitrogen, which is the filling gas of the ionisation chambers used. Because the mass energy-absorption coefficient is practically constant, it can be ignored in equation (2). [4, 5]

Assemblies, which have off-reactor cycles, have effectively a longer cooling time than the time between the measurement and evacuation date. In these measurements four assemblies, #13624432, #22421319, #13632649 and #13624532, had off-reactor cycles.

The effect of off-reactor cycles on the ^{137}Cs activity was investigated with PYVO calculations. The ^{137}Cs activity was calculated in the cases when an assembly has been irradiated in sequential one-year cycles and when an assembly has a varying number of sequential one-year off-reactor cycles between the irradiation cycles. The assumption of a linear development of the burnup vs. the irradiation cycles was made.

The ratio of the ^{137}Cs activity with off-cycles to the ^{137}Cs activity without off-cycles was correlated with the ratio of irradiation cycles after the off-cycles to the total number of irradiation cycles according to equation (3). The number of off-reactor cycles was kept constant.

$$\frac{A_{37,j,o,h}}{A_{37,i}} = p + q * \frac{h}{i}, \qquad (3)$$

where $A_{37,i}$ denotes the calculated ^{137}Cs activity without off-cycles,

$A_{37,j,o,h}$ denotes the calculated ^{137}Cs activity with off-cycles,

i is the total number of irradiation cycles,

j is the number of irradiation cycles before off-reactor cycles,

h is the number of irradiation cycles after off-reactor cycles (i = j + h),

o is the number of off cycles and

p and q denote off cycles number dependent parameters received from the fit.

The parameters received from the fits corresponding to different numbers of off-cycles are shown in Table III. Correlation curves with five different numbers of off-cycles are presented in Figure 3.

Utilising Table III, the parameters p and q
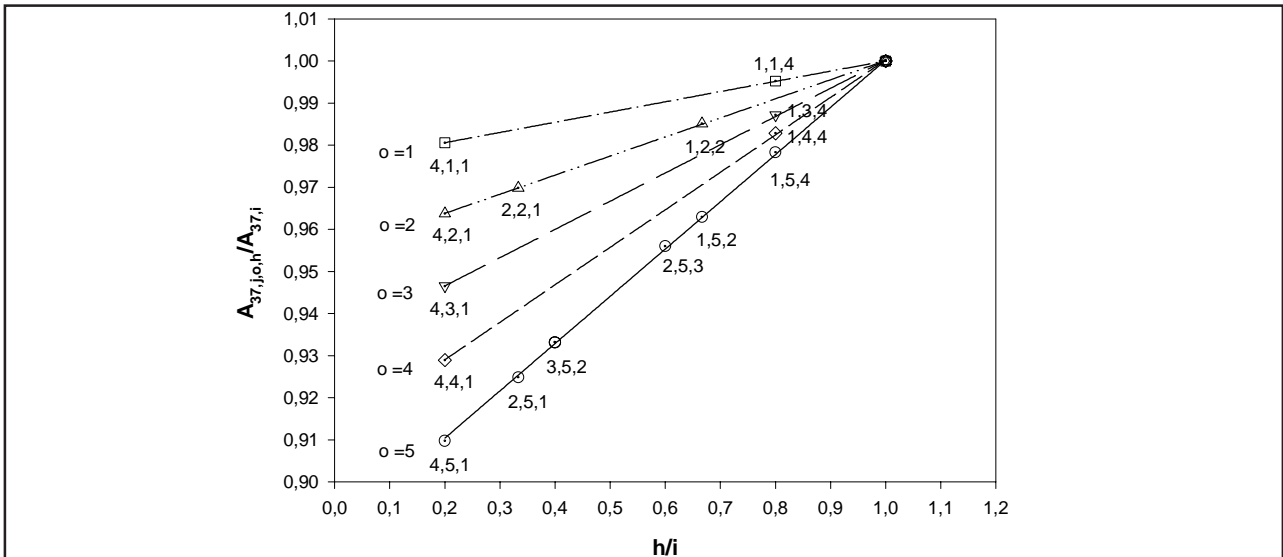
Figure 3. *Calculated* ^{137}*Cs ratio vs. the ratio of irradiation years after off-cycles to the total number of irradiation years. The number of off-cycles is varied from 1 to 5. Irradiation years before the off cycles, the number of off cycles and irradiation years after off cycles (j,o,h) are also shown for the data points.*
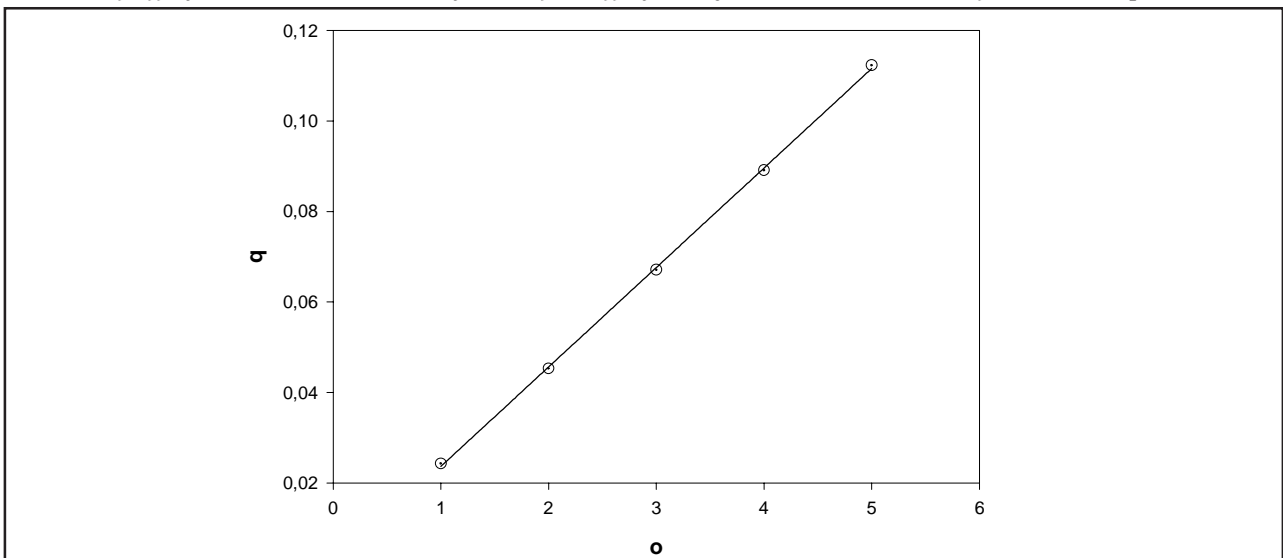
Figure 4. *Slope of equation (3) vs. the number of off cycles.*
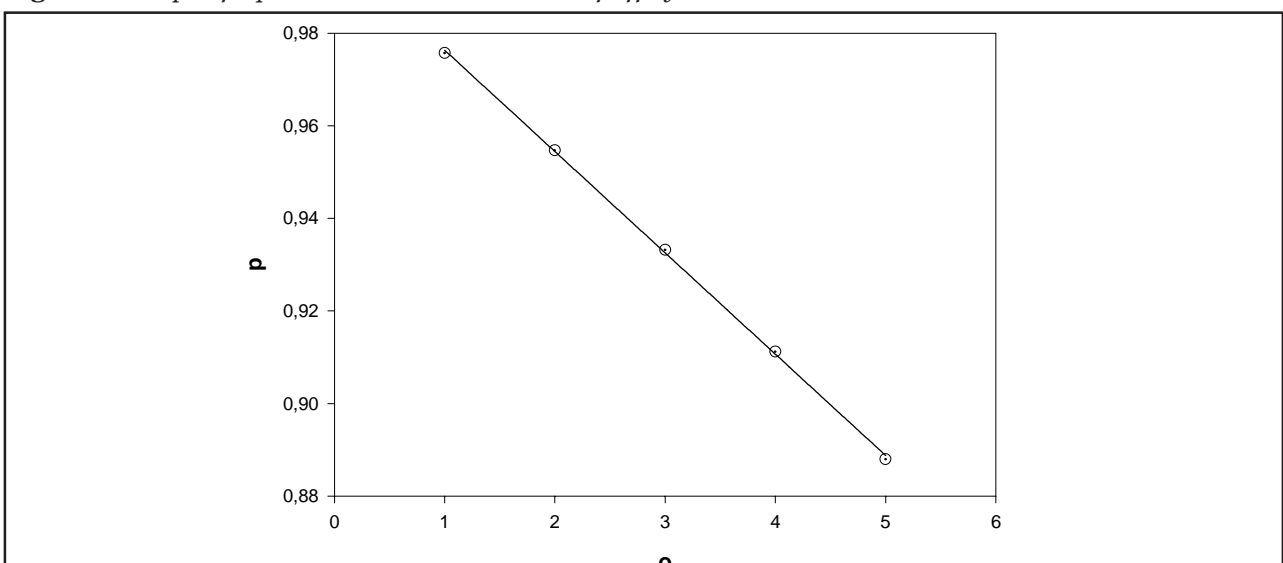
Figure 5. *Zero crossover of equation (3) vs. the number of off cycles.*

were correlated linearly to the number of off cycles according to the equations

$$q = c_1 + c_2 * o \qquad (4)$$

and

$$p = d_1 + d_2 * o , \qquad (5)$$

where c_1, c_2, d_1 and d_2 denote the parameters received from the fit and o denotes the number of off-reactor cycles.

Both the slope and zero crossover of these curves seem to be linearly dependent on the number of off cycles. The values of the parameters received from the fits are $c_1 = 0.0017 \pm 0.0008$, $c_2 = 0.0220 \pm 0.0002$, $R^2 = 0.9997$ in equation (4) and $d_1 = 0.9982 \pm 0.0008$, $d_2 = -0.0219 \pm 0.0002$ and $R^2 = 0.9996$ in equation (5).

For the gross gamma, the recipe obtained for off-reactor cycle correction is

$$G_{37,i} = \frac{G_{37,j,o,h}}{1 - 0.022 * o * \frac{j}{i} - 0.002 * \frac{j}{i}} , \qquad (6)$$

where $G_{37,i}$ denotes gross gamma corrected for off-cycles,

$G_{37,j,o,h}$ denotes the measured gross gamma with off-cycles,

i stands for the total number of irradiation cycles,

j stands for the number of irradiation cycles before off-reactor cycles,

h stands for the number of irradiation cycles after off-reactor cycles and

o stands for the number of off cycles.

The correction factor increases as the number of off cycles increases or when h/i decreases. The off cycle correction recipe can be used for assemblies independently of the initial enrichment value or of the total burnup.

The gamma spectrometrically measured ^{137}Cs intensity was corrected for off-reactor cycles according to the same method as that presented for gross gamma in equation (6).

Another way to approach the effect of off cycles is to use the linear correlation of ^{137}Cs activity to burnup. If an assembly has been irradiated in sequential cycles, the ^{137}Cs activity correlates linearly to burnup according to equation

$$A_{37,i} = k * B , \qquad (7)$$

where B stands for the burnup and
k represents the proportionality coefficient received from the fit.

If an assembly has off cycles, the ^{137}Cs activity on the evacuation date is

$$A_{37,j,o,h} = k * \left(e^{-0.0230511*t} * B_j + B - B_j \right), \qquad (8)$$

where t denotes the off cycle time in years and
B_j denotes the burnup before the off cycles.

The constant 0.0230511 is the decay constant of ^{137}Cs in inverse years. The ratio of ^{137}Cs activity with off cycles to ^{137}Cs activity without off cycles can be calculated using equations (7) and (8)

$$\frac{A_{37,j,o,h}}{A_{37,i}} = 1 - \left(1 - e^{-0.0230511*t}\right) * \frac{B_j}{B} . \qquad (9)$$

If the burnup is developed linearly to the irradiation cycles, and the total time of off cycle is much less than the half-life of ^{137}Cs, a linear approximation can be used for the exponential function and the recipe for off cycle correction get the form

$$G_{37,i} = \frac{G_{37,j,o,h}}{1 - 0.0230511 * o * \frac{j}{i}} . \qquad (10)$$

The two methods, the linear fitting of the results obtained by the PYVO calculations, equation (6), and the physical approach, equation (10) yield essentially the same dependence on the off-reactor cycles. The largest difference is only 0.2 % among the measured assemblies which is for #13624432 with five off cycles. The physical approach gives additionally a physical significance to the numerical constant in those two equations.

It is important to note that the off-cycle effect does not decay away during the storage of the spent assembly, but is a permanent property depending only on the irradiation history.

4.1.2 Correlation of ^{137}Cs signal to burnup

A linear fit of the gamma spectrometrically measured ^{137}Cs peak intensity vs. burnup according to

$$A_{37} = k * B \qquad (11)$$

is shown in Figure 6.

The ^{137}Cs activity was calculated for all meas-

Table IV. *Parameters of experimental and calculated ^{137}Cs signal vs. burnup fit.*

	k	σ_k	σ_k/k	R^2
Experimental	8.6277	0.0828	0.0096	0.979
PYVO	8.6269	0.0095	0.0011	1.000

ured assemblies using the PYVO program. The calculated ^{137}Cs activities were scaled to correspond to the spectrometrically measured ^{137}Cs peak intensity. The parameters of both fits are compared in Table IV.

In addition, the 90 % prediction interval for the measured ^{137}Cs peak intensity vs. burnup curve is shown in Figure 6. This 90 % confidence interval for the population describes the range where data values will fall at 90 % probability for repeated measurements. This prediction interval is called the *error corridor* in the remainder of this report. The absolute width of the error corridor is ± 24 cps, equal to ±6.5 % of the maximum value of 377 cps corresponding to the maximum burnup of 43.67 MWd/kg.
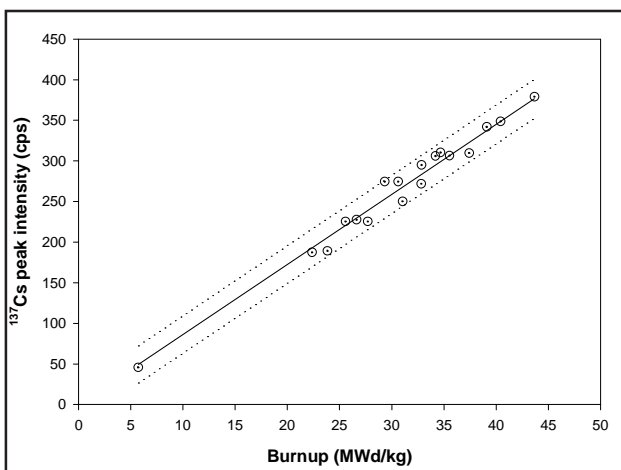
4.1.3 Correlation of gross gamma to burnup

The gross gamma signal of the measured VVER assemblies was correlated to the burnup according to

$$G_{37} = k' * B, \tag{12}$$

see Figure 7.

The parameters of the fits to the experimental data and to the corresponding data calculated with PYVO are shown in Table V. As expected, the

Figure 6. *Measured ^{137}Cs intensity vs. burnup. Dotted lines describe the error corridor.*

Table V. *Parameters of calculated and experimental gross gamma vs. burnup fit.*

	k'	$\sigma_{k'}$	$\sigma_{k'}/k'$	R^2
Experimental	18.7047	0.1056	0.0056	0.992
PYVO	18.7037	0.0205	0.0011	1.000

gross gamma correlates to the burnup better than the gamma spectroscopically measured ^{137}Cs peak intensity. The explanation is that the gross gamma is less sensitive to positioning error than the spectrometrically measured ^{137}Cs peak intensity. This is explained more in detail in ref. [1]. The correction for two nuclides, ^{134}Cs and ^{106}Ru/Rh, seems to be sufficient even for cooling times as short as 2.7 years.

The absolute width of the error corridor is ± 30 units for VVER assemblies, equal to ±3.9 % of the maximum value of 817 units corresponding to the maximum burnup of 43.67 MWd/kg. The gross gamma data measured in Olkiluoto indicate that the corresponding error corridor for BWR assemblies is about twice as wide as it is for VVER assemblies [1]. The correlation is better for VVER assemblies than for BWR assemblies even if the measured VVER assemblies had shorter cooling times than the measured BWR assemblies and the gross gamma signal was corrected for the same nuclides in both cases. The correlation coefficient is 0.963 for BWR assemblies and 0.992 for VVER
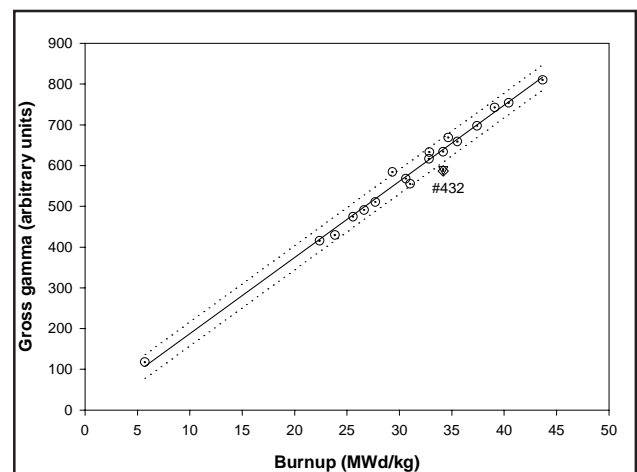
Figure 7. *Gross gamma signal vs. burnup. The circles represent the experimental points. Dotted lines describe the error corridor of the experimental data. The diamond represents the experimental result for assembly #13624432 without correction for off-reactor cycles. The triangle down represents the corresponding case for PYVO data. The corrected experimental point lies right above the uncorrected one.*

assemblies [1]. This implies that boiling conditions in the reactor may increase the scatter of data points.

Four measured assemblies have off-reactor cycles: #13624432, #22421319, #13632649 and #13624532. The effect of off-reactor cycle correction to the gross gamma signal has been demonstrated in Table VI and in Figure 7. The assembly #13624432 has been irradiated in three cycles. After the first two cycles it had five off-reactor cycles. Had the off-cycle correction not been applied, the measured data point would have fallen outside the error corridor. Applying the off-cycle correction makes it to fit perfectly on the correlation curve. The off-cycle correction may be important for correct burnup verification.

4.2 Neutron measurements

Correlation between the neutron counts from the bare fission chambers and the neutron counts from the Cd-wrapped fission chambers was perfectly linear. Also the zero crossover value was zero. Cd-wrapped fission chamber signal is used in all following correlations.

4.2.1 Corrections applied to neutron signal

The measured neutron data have been corrected for the share of ^{244}Cm neutrons, for the decay of ^{244}Cm and for enrichment variation.

The share of ^{244}Cm neutrons of the total neutron source is derived from the results calculated with the PYVO program. It varied from 4 % to 97 % among the measured VVER assemblies. It increases when the burnup or cooling time increases or when the initial enrichment decreases.

Because the spent fuel assemblies have different initial enrichments, the measured neutron data have been corrected to a certain reference enrichment value. An enrichment correction method based on the calculations made with the SAS2H/ORIGEN-S program to the measured neutron data of BWR assemblies is introduced in ref. [1]. The corresponding recipe for VVER assemblies was calculated with the PYVO program. The enrichment was varied from 1.6 % to 4.2 % and the burnup from 15 MWd/kg to 45 MWd/kg. The irradiation time was adjusted in such a way that

Table VI. *Effect of off cycles in gamma signal.*

Ass. ID	*j,o,h*	off cycle correction factor
13624432	2,5,1	1.080
22421319	2,2,1	1.031
13632649	2,1,1	1.016
13624532	1,1,2	1.008

the average power of the assemblies was 34.01 kW/kg. The calculated ^{244}Cm neutron sources at discharge are shown in Table A2.I in Annex 2.

To obtain a recipe for the enrichment correction the ^{244}Cm neutron source was correlated to the initial enrichment at a constant burnup. The ^{244}Cm neutron source was correlated to the initial enrichment according to the equation

$$\ln N_O = s' - r * IE \qquad (13)$$

where N_O denotes the ^{244}Cm neutron source at discharge

IE denotes the initial enrichment and

s' and r denote burnup dependent parameters received from the fit.

The parameters received from the fits corresponding to different burnup values are shown in Table VII. Correlation curves with seven different burnup values are shown in Figure 8.

The parameter r in Table VII was correlated to the burnup according to the equation

$$r = t_1 + t_2 * B \qquad (14)$$

where t_1 and t_2 denote the paremeters received from the fit and

B denotes the discharge burnup.

The values of the parameters received from the fit are t_1 = (1.1509 ± 0.0060) %$^{-1}$, t_2 = (-0.0125 ± 0.0002) (%*MWd/kg)$^{-1}$ and R^2 = 0.9989, see Figure 9.

The enrichment correction recipe for VVER assemblies is

$$N_R = N * e^{(1.1509-0.0125*B)*(IE-IE_R)} , \qquad (15)$$

where N_R denotes the ^{244}Cm neutron count rate of an assembly as corrected to the reference enrichment and N denotes the measured ^{244}Cm neutron count rate of an assembly. IE_R denotes the reference enrichment, which was chosen to be 3.6 %, IE denotes the operator declared initial enrichment of the assembly and B denotes the discharge burnup.

Table VII. *Parameters of the ^{244}Cm neutron yield vs. initial enrichment fits with different burnup values.*

Burnup (MWd/kg)	s´	$\sigma_{s´}$	r	σ_r	R^2
15	18.8826	0.0774	−0.9705	0.0257	0.9916
20	20.1344	0.0620	−0.8989	0.0206	0.9937
25	21.0311	0.0480	−0.8336	0.0160	0.9956
30	21.7025	0.0352	−0.7713	0.0117	0.9973
35	22.2173	0.0235	−0.7106	0.0078	0.9985
40	22.6173	0.0135	−0.6511	0.0045	0.9994
45	22.9303	0.0060	−0.5928	0.0020	0.9999
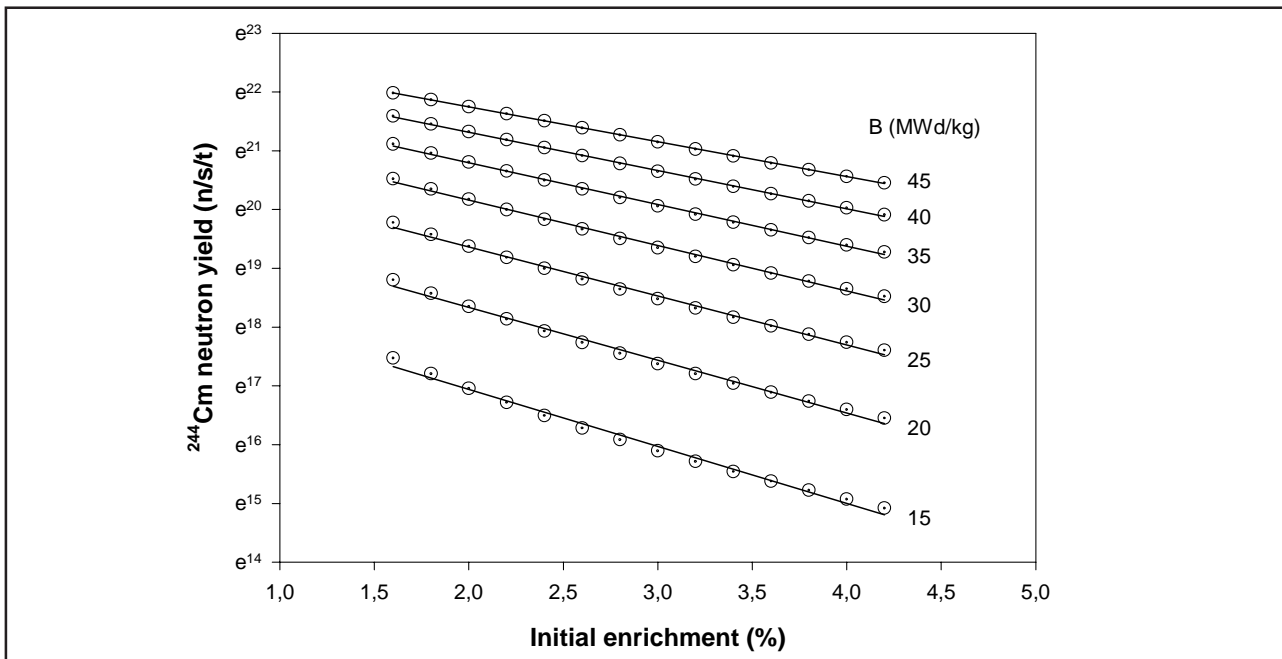
Figure 8. *Calculated ^{244}Cm neutron source vs. initial enrichment. Burnup is varied from 15 MWd / kg to 45 MWd / kg.*
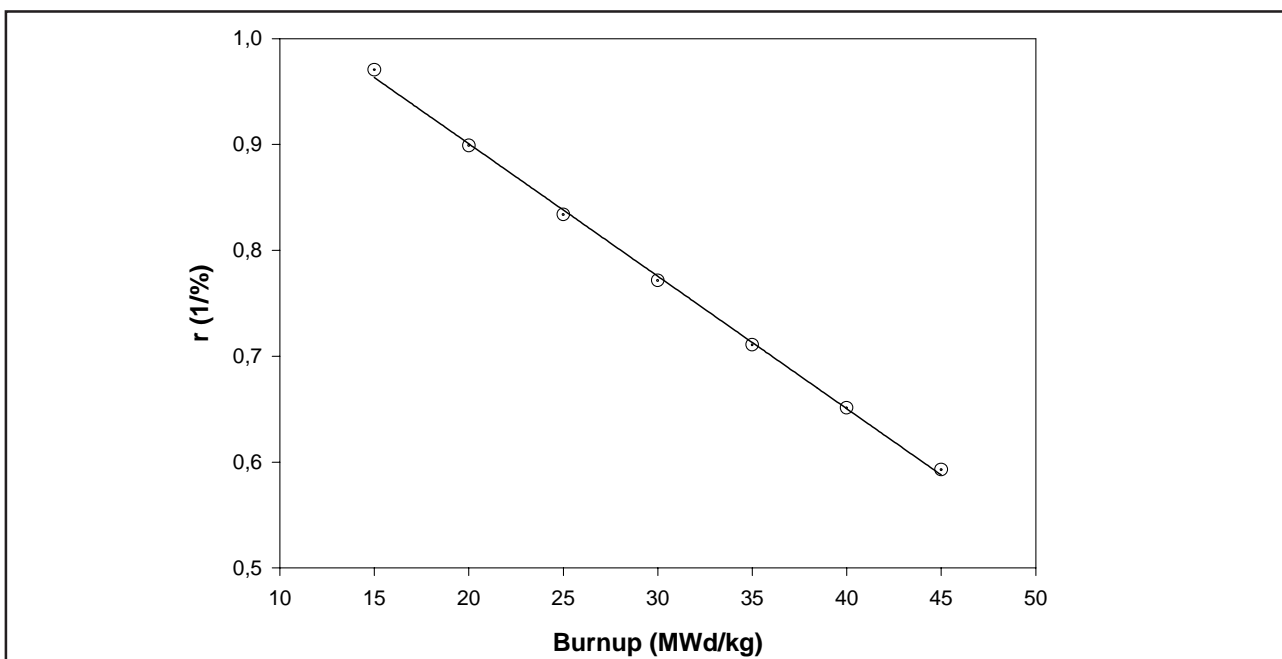
Figure 9. *Coefficient r vs. burnup.*

The effect of off-reactor cycles on ^{244}Cm neutrons has also been studied with PYVO calculations, see Figure 10. The effect was insignificant in the off cycle combinations of the measured assemblies. The importance of the off-reactor cycles correction increases rapidly when h/i becomes very low and the number of off cycles increase. I.e. the correction may become important for four total irradiation cycles if the last cycle has been irradiated separately with at least three years off the reactor before the last cycle or for five total irradiation cycles if the last cycle has been irradiated separately with at least two years off the reactor before the last cycle.

4.2.2 Correlation of neutron signal to burnup

Neutrons were correlated to burnup according to the equation

$$\log_{10}(N) = \alpha + b * \log_{10}(B), \tag{16}$$

where N is the measured neutron count rate. α and b are parameters received from the fit, see Figure 11. Equation (16) is equivalent with the neutron-to-burnup correlation given in equation (1). The parameter b obtained in these fits corresponds to the power indicated in equation (1). The results of the fits to the experimental and PYVO
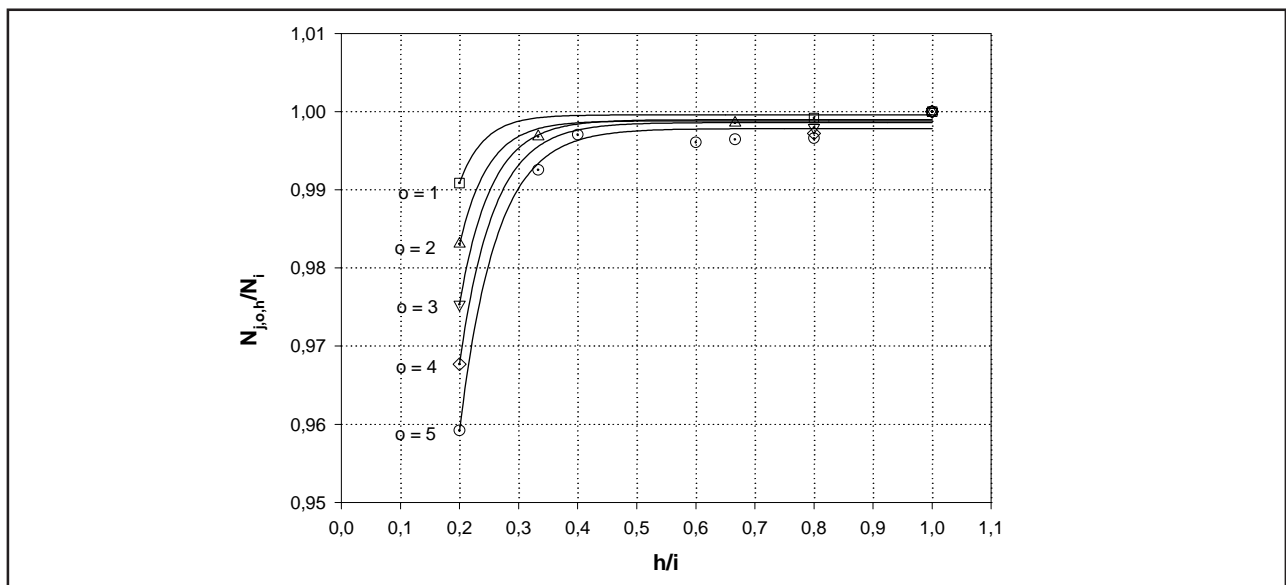

Figure 10. *The dependence of ^{244}Cm neutrons on off-reactor cycles.*
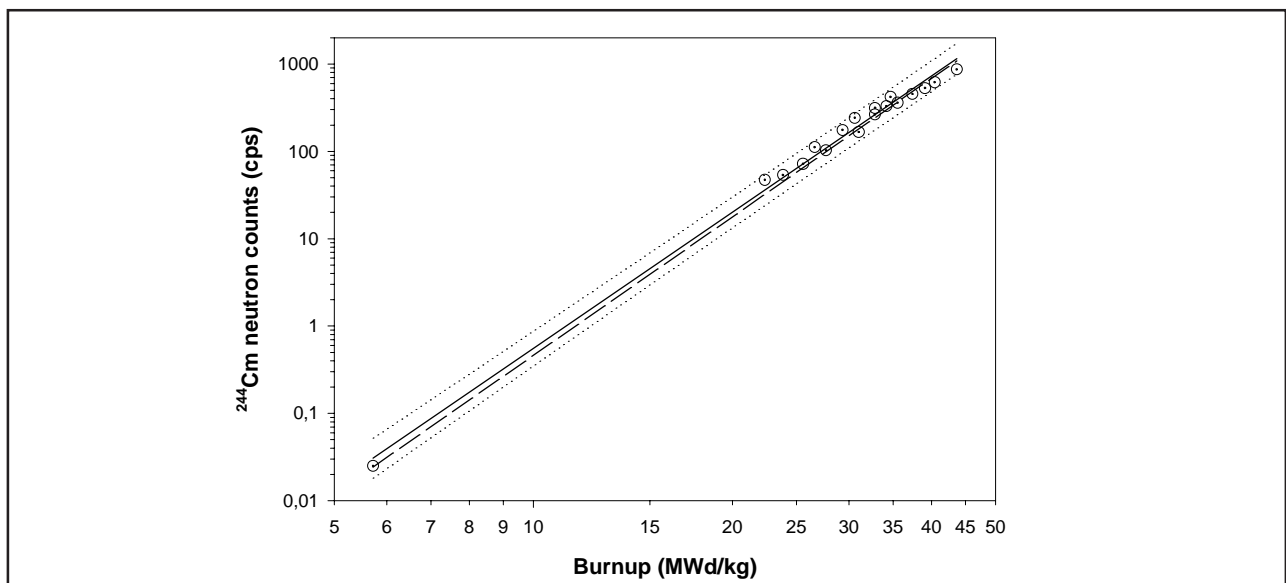

Figure 11. *^{244}Cm neutrons vs. burnup. The circles represent the experimental values and the solid line represents the fit to the experimental data. Dotted lines limit the error corridor. The dashed line represents the fit to the PYVO data.*

Table VIII. *Neutrons vs. burnup. Parameters of equation (16). UL and LL indicate the parameters of the upper and lower limit of the error corridor (Figure 11).*

	Enrichment correction	α	σ_α	b_α	σ_b	R^2
PYVO	yes	−5.60	0.07	5.27	0.05	0.999
Experimental	yes	−5.44	0.15	5.18	0.10	0.994
UL	yes	−5.17		5.12		
LL	yes	−5.71		5.24		
Experimental	no	−5.06	0.45	5.02	0.30	0.945

calculated data are shown in Table VIII. The error corridor is ± 5.6 % at high burnup values and ± 15 % at low burnup values, see Figure 11.

The slope of the neutrons vs. burnup curve is higher for VVER assemblies than for BWR assemblies.

The measured VVER assemblies have only two different initial enrichment values, 2.4 % and 3.6 %. The enrichment correction improves the fit making it possible to correlate all data points in the same fit, see Table VIII. An alternative option would have been to correlate the assemblies with enrichments 2.4 % and 3.6 % separately.

4.2.3 Correlation of neutron signal to gamma signal

Neutrons were correlated to spectroscopically measured ^{137}Cs peak intensity and the gross gamma according to the equations

$$\log_{10}(N) = \alpha' + b' * \log_{10}(A_{37}), \qquad (17)$$

Table IX. *Neutrons vs. gamma spectrometrically measured ^{137}Cs peak intensity. Parameters of equation (17). UL and LL as in Table VII (Figure 12).*

	α'	$\sigma_{\alpha'}$	b'	$\sigma_{b'}$	R^2
PYVO	−10.71	0.11	5.34	0.05	0.999
Experimental	−9.64	0.27	4.92	0.11	0.992
UL	−9.27		4.85		
LL	−10.00		4.98		

$$\log_{10}(N) = \alpha'' + b'' * \log_{10}(G_{37}), \qquad (18)$$

where N is the measured neutron count rate. α', b', α'' and b'' are parameters received from the fit. The results are shown in Tables IX and X and plotted in Figures 12 and 13.

The error corridors are shown in Figures 12 and 13. The error corridor width of the ^{244}Cm neutrons vs. gross gamma curve is about ± 7.2 % at high gross gamma values and ± 20 % at low gross gamma values. The corresponding error corridor for ^{244}Cm neutrons vs. ^{137}Cs peak intensity curve is about ± 6.5 % at high ^{137}Cs peak
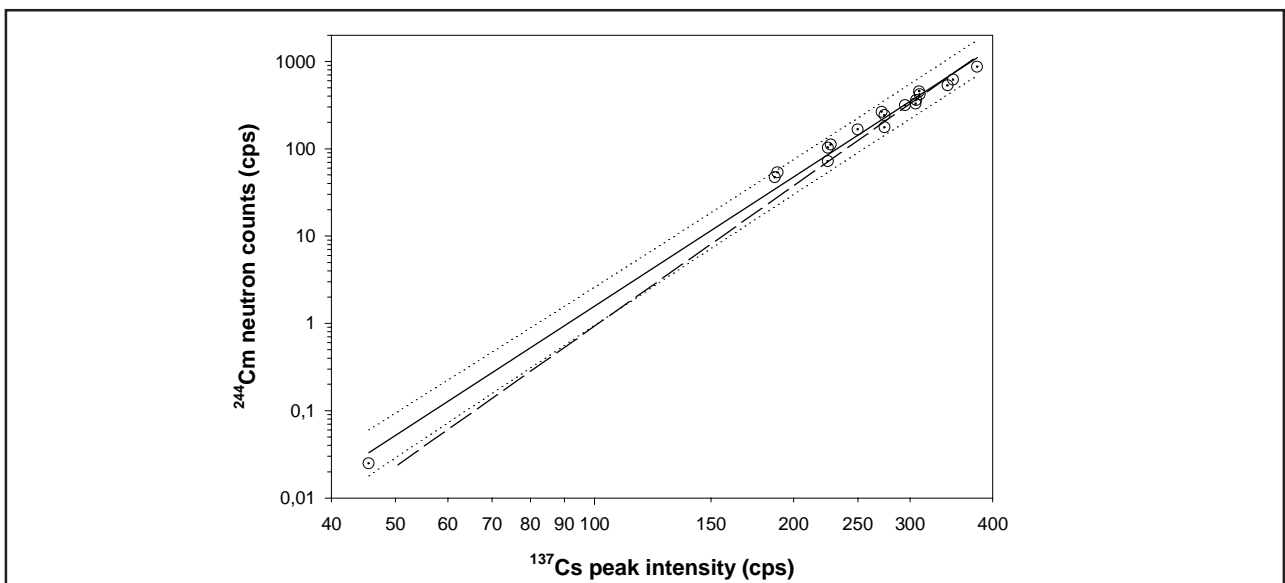

Figure 12. *^{244}Cm neutrons vs. the ^{137}Cs peak intensity. The circles represent the experimental values and the solid line represents the fit to the experimental data. Dotted lines describe the error corridor. The dashed line represents the fit to the PYVO data.*

Table X. Neutrons vs. gross gamma. Parameters of equation (18). UL and LL as in Table VII (Figure 13).

	α''	$\sigma_{\alpha''}$	b''	$\sigma_{b''}$	R^2
PYVO	−12.51	0.13	5.34	0.05	0.999
Experimental	−12.55	0.38	5.37	0.14	0.990
UL	−12.11		5.29		
LL	−13.00		5.45		

intensity values and ± 17 % at low ^{137}Cs peak intensity values. All assemblies, both PK and TBC assemblies, are inside the error corridors when neutrons are correlated to gross gamma or to ^{137}Cs peak intensity. The PYVO calculations give somewhat different power parameters when correlating neutrons to burnup and to ^{137}Cs activity (5.27 vs. 5.34). This difference may not be significant. The best experimental correspondence with the PYVO calculations is obtained by correlating the measured neutrons to the gross gamma, see Table X.

4.3 Sensitivity to vertical positioning

It was found out in the analysis of the Olkiluoto measurements that burnup profile variation and positioning in axial direction are no considerable error source at least inside about one metre interval in the central part of an assembly. [1] The same kind of study was performed also in the Loviisa campaign. The measurements were performed at three heights: at the mid-point, 500 mm above the mid-point and 500 mm below the mid-point.

All measured data points have been taken into consideration in the following fits. All corrections mentioned in sections 4.1 and 4.2 have been made to the measured data. The analysis was made using the neutron counts from Cd-wrapped fission chambers, because the correlation between the Cd-wrapped and bare neutron channels was found to be independent of the height. The measured raw data are shown in Table A1.I in Annex 1.

The ^{244}Cm neutron counts vs. gross gamma curve and its error corridor at the mid-point is shown in Figure 14. Also the data points measured at the lower and higher heights are included in Figure 14. The data points of all three measurement heights are inside the error corridor. This confirms the conclusion of the Olkiluoto analysis that the positioning in axial direction is not a measurable error source as far as the measurement takes place within one metre interval about the centre of an assembly. Also the values of the parameters in the case when the data points measured at all three heights are included in the same fit are shown in Table XV Axial profile variations between VVER assemblies were not investigated. Only one assembly was scanned axially in Loviisa. See section 5. However, no indication that variations in axial profiles could be a
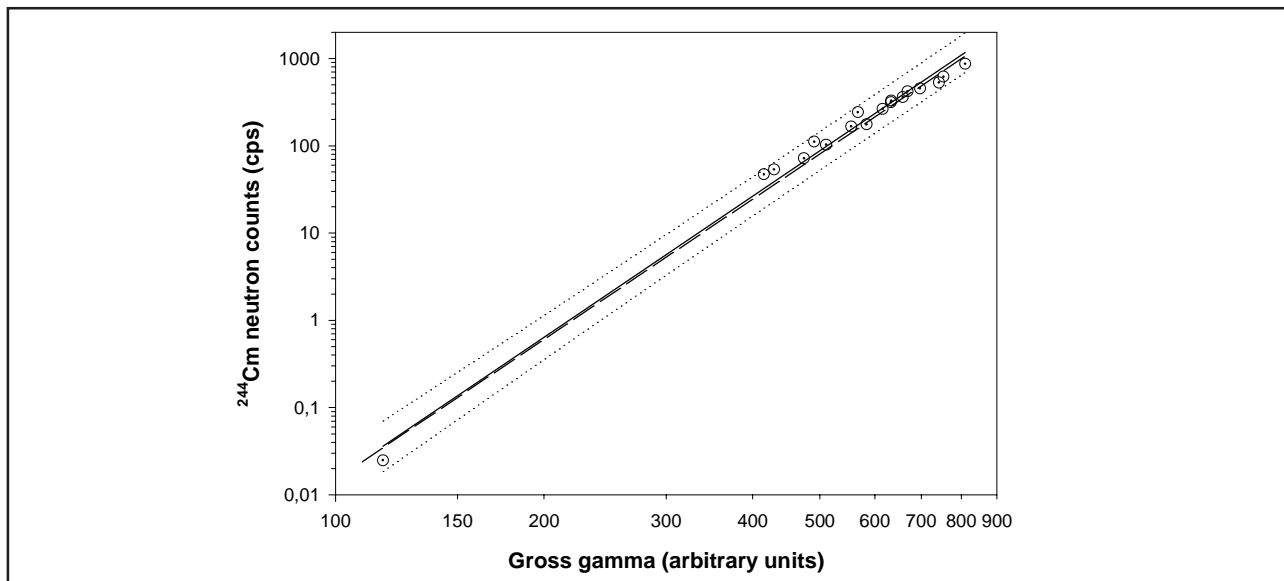

Figure 13. ^{244}Cm neutrons vs. gross gamma. The circles represent the experimental values and the solid line represents the fit to the experimental data. The dotted lines describe the error corridor. The dashed line represents the fit to the PYVO data.

Table XI. *Parameters the* ^{137}Cs *peak intensity vs. burnup fit.*

	k	σ_k	σ_k/k	R^2
LOW	8.20	0.09	0.011	0.973
MID	8.63	0.08	0.010	0.979
HIGH	8.34	0.08	0.009	0.979

Table XII. *Parameters of the gross gamma vs. burnup fit.*

	k''	$\sigma_{k''}$	$\sigma_{k''}/k''$	R^2
LOW	18.11	0.14	0.008	0.986
MID	18.70	0.11	0.006	0.992
HIGH	18.11	0.12	0.007	0.989

Table XIII. *Parameters of the* ^{244}Cm *neutron counts vs. burnup fit.*

	α	σ_α	b	σ_b	R^2
LOW	−5.42	0.16	5.13	0.11	0.993
MID	−5.44	0.15	5.18	0.10	0.994
HIGH	−5.39	0.14	5.12	0.10	0.995

Table XIV. *Parameters of the* ^{244}Cm *neutron counts vs.* ^{137}Cs *peak intensity.*

	α'	$\sigma_{\alpha'}$	b'	$\sigma_{b'}$	R^2
LOW	−9.45	0.27	4.86	0.11	0.992
MID	−9.64	0.27	4.92	0.11	0.992
HIGH	−9.30	0.24	4.79	0.10	0.993

Table XV. *Parameters of the* ^{244}Cm *neutron counts vs. gross gamma.*

	α''	$\sigma_{\alpha''}$	b''	$\sigma_{b''}$	R^2
LOW	−11.58	0.24	5.02	0.09	0.995
MID	−12.55	0.38	5.37	0.14	0.990
HIGH	−11.85	0.27	5.13	0.10	0.994
All heights	−12.27	0.19	5.23	0.07	0.991

significant error source was found among VVER assemblies in ^{244}Cm neutron counts vs. gross gamma curve either.

The ^{137}Cs peak intensity and gross gamma were correlated to burnup at all three heights. The results are shown in Tables XI and XII.

The ^{244}Cm neutron counts were correlated to the burnup, ^{137}Cs peak intensity and gross gamma, see Tables XIII, XIV and XV.

4.4   Comparison of neutron curves

Whether the neutrons correlate best with the burnup, ^{137}Cs peak intensity or gross gamma can not be concluded for VVER assemblies with a few years' cooling time. Because of short cooling time their gross gamma signal includes additional contribution originating from other isotopes than those accounted for in the corrections to the gross
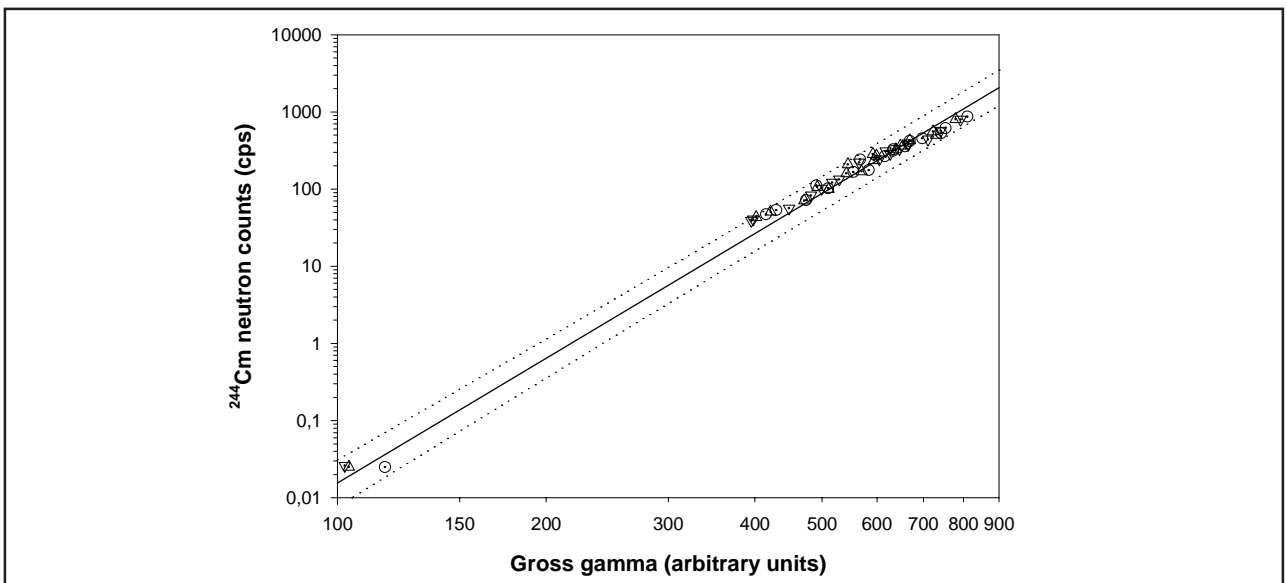

Figure 14. *^{244}Cm neutron counts vs. gross gamma at three heights. Triangles up correspond to height 500 mm above the mid-point. Circles and solid regression line correspond to the mid-point. Triangles down correspond to height 500 mm below the mid-point. Dotted lines represent the error corridor corresponding to the regression line at the mid-point.*

gamma signal. This degrades the neutrons vs. gross gamma correlation. However, the correlation of the neutrons to the gross gamma is expected to become better with longer cooling time when parasitic gamma emitters have decayed off. This may be important concerning the final disposal of spent fuel, because the assemblies to be disposed of are expected to have long cooling time.

The correspondence between the fits to the measured data and to the data calculated with PYVO is quite complete when neutrons are correlated to the gross gamma or to the burnup, see Figures 11 and 13. When neutrons are correlated to the gamma spectrometrically measured ^{137}Cs peak intensity the results received from the fit deviate significantly from the corresponding results of the calculated data, see Figure 12. This indicates that the gamma spectrometrically measured ^{137}Cs peak intensity may contain some systematic error.

4.5 Importance of averaging the measurement data

The ^{244}Cm neutrons were correlated to gross gamma according to equation (18) without averaging over two azimuthal angle values. The results are shown in Table XVI and Figure 15. The width of the error corridor does not change with averaging

Table XVI. *Neutrons vs. gross gamma without averaging over two sides of an assembly. UL and LL as in Table VIII.*

	α''	$\sigma_{\alpha''}$	b''	$\sigma_{b''}$	R^2
Experimental	−12.54	0.28	5.36	0.10	0.988
UL	−12.19		5.32		
LL	−12.89		5.41		

over the azimuthal angle. This backs up the conclusion made from the measurements in Olkiluoto, that the width of the error corridor is primarily determined by variation of the factors affecting the gamma and neutron emission of different assemblies during irradiation. The random factors attributed to the measurement itself, like positioning accuracy and counting statistics, do not significantly affect the accuracy of an individual measurement. [1] The only measurement point that falls outside the error corridor belongs to the assembly #13648120 with a very low burnup value of 5.7 MWd/kg. This indicates that a better measurement statistics might be needed to improve the quality of data of very low burnup assemblies. In order to average real asymmetries due to asymmetrical irradiation conditions, measuring the neutron signal and gross gamma from all sides of an assembly may be important. This would require three measurements with 60° rotations per VVER assembly.
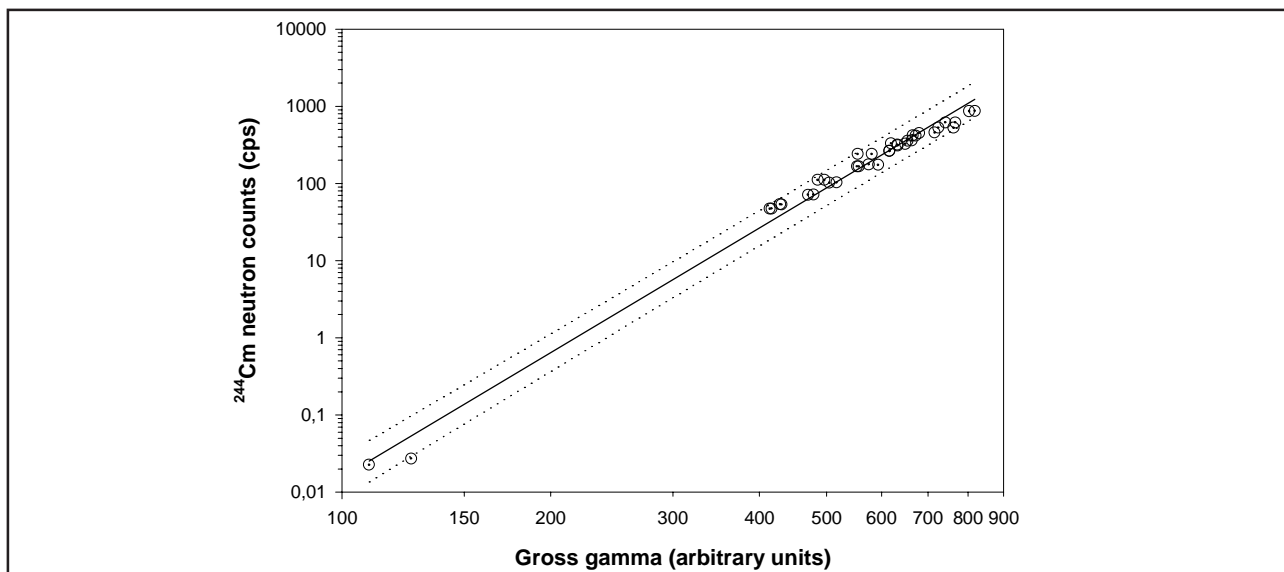
Figure 15. *^{244}Cm neutrons vs. gross gamma without averaging over two azimuthal angles. Dotted lines describe the error corridor.*

5 AXIAL SCANNING

The measured axial scanning results of assembly #13640621 are shown in Figures 16 and 17. Figure 16 shows that the gross gamma signal seems to follow the axial distribution of gamma spectrometrically measured ^{137}Cs peak intensity everywhere except in the bottom and top part of the assembly. Top and bottom structures of the assembly are made of stainless steel and the active length of a fuel pin is 2420 mm [6]. The impurities in stainless steel, especially cobalt, activate during irra-

diation. The gross gamma signal does not approach zero at the top and bottom part of the assembly, because of these parasitic gamma emitters.

As in the measurements performed in Olkiluoto, the axial distribution of the neutron emission seems to be almost independent of whether the measurement is taken with bare or Cd-wrapped fission chambers, see Figure 17. The raw data of these measurements are shown in Table A1.II in Annex 1.
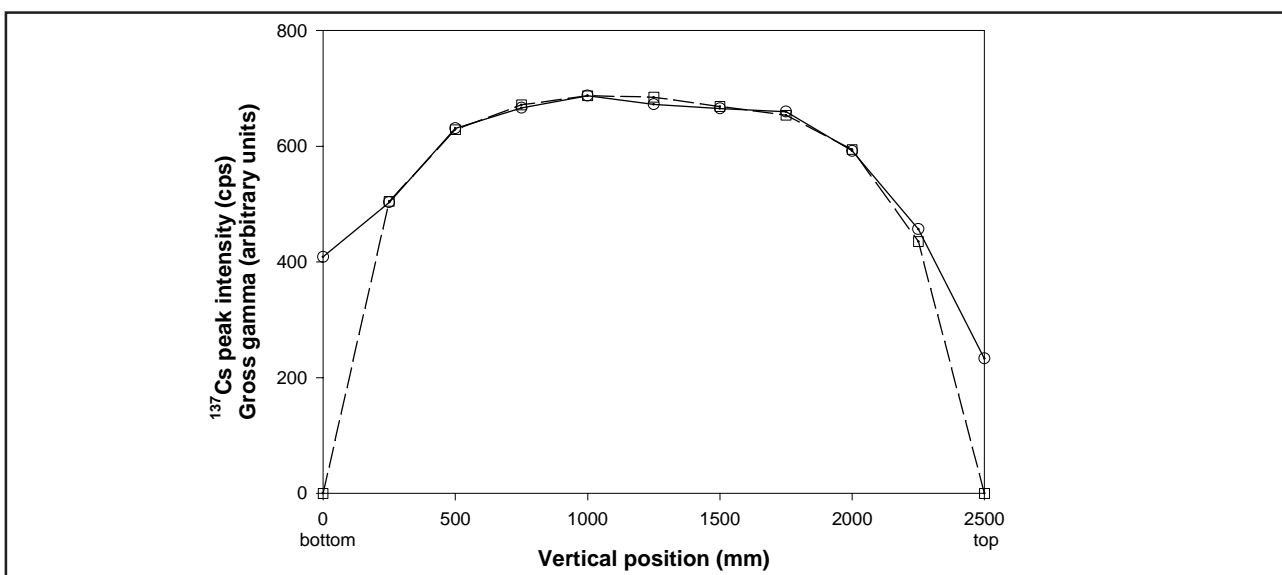
Figure 16. Axial scanning of assembly #13640621. Squares and dashed line represent the ^{137}Cs peak intensity. Circles and solid line represent the gross gamma signal.
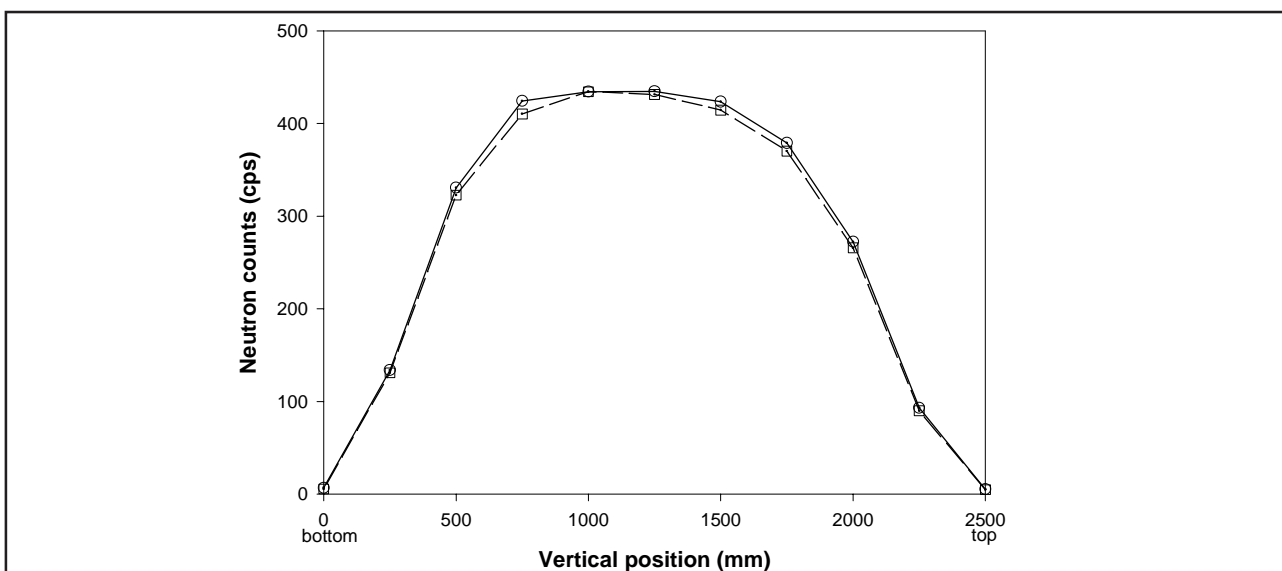
Figure 17. Axial scanning of assembly #13640621. Squares and dashed line represent the neutron intensity from Cd-wrapped fission chambers. Circles and solid line represent the neutron intensity from bare fission chambers.

6 CONCLUSION

The contribution of other gamma emitting nuclides than ^{137}Cs was eliminated from the gross gamma signal using gamma-spectroscopic data. The main parasitic contributors identified in the spectra were ^{134}Cs and ^{106}Ru/Rh. Correction for these nuclides was sufficient even if many assemblies had only a few years of cooling time. The gross gamma signal of VVER assemblies seems to correlate better to burnup than the gross gamma signal of BWR assemblies according to the measurements performed in Loviisa and Olkiluoto.

Four measured assemblies have off-reactor cycles between irradiation cycles. Because ^{137}Cs decays during the off cycles the ^{137}Cs signal was corrected to correspond to the history of sequential irradiation cycles with help of PYVO program. It seems that off cycle correction may be very important for burnup verification purposes. The assemblies, which have off cycles, are special cases whose ^{137}Cs signal may be too low without the off cycles correction. This could mislead an inspector to make a conclusion that the operator declared burnup would be wrong. The off cycle correction may save both money and time by making it possible to avoid additional inspections of these assemblies.

The same corrections were made to the measured neutron data as in the analysis of measurements performed in Olkiluoto. The share of the ^{244}Cm neutron source out of the total neutron counts is derived from the results calculated with PYVO. It varied from 4 % to 97 % among the measured assemblies. It increases when the burnup or cooling time increases or when the initial enrichment decreases. PYVO can be considered as an important tool for future measurements as the share of ^{244}Cm neutrons of the total neutron counts has to be calculated separately for each assembly at each measurement campaign.

The enrichment correction recipe to neutron data was calculated for VVER assemblies using the PYVO program. However, the enrichment correction is not as essential as it was in the analysis of the Olkiluoto campaign where the enrichment variation was large among the measured BWR assemblies. Because the initial enrichment of the measured VVER assemblies is either 2.4 % or 3.6 %, the neutron data could have been analysed separately for these two enrichments. Including all assemblies in one correlation curve was possible by correcting the neutron data to a reference enrichment value of 3.6 %. In any case, the VVER assemblies may probably have more diverse enrichments in the prospective measurements, which would make the enrichment correction important also for VVER assemblies. These corrections were found to improve the correlation of neutrons both to the declared burnup and to the measured burnup indicators. Neutron multiplication has not been taken into consideration in the analysis.

The effect of off-reactor cycles on ^{244}Cm neutron counts was investigated with help of PYVO program. The effect was insignificant in the off cycle combinations of the measured assemblies. The importance of the off cycle correction increases rapidly with the increasing number of off cycles. Also the later the off cycles are in the irradiation history the bigger effect they have to the ^{244}Cm neutron signal. In extreme cases the off cycles may affect significantly also the ^{244}Cm neutron signal.

The ^{244}Cm neutron source and ^{137}Cs activity were calculated for all measured assemblies using the PYVO program. The correspondence between the measured and calculated results seems to be very good when the ^{244}Cm neutrons are correlated to the burnup or to the gross gamma.

^{244}Cm neutrons correlate almost as well to the gross gamma as to the burnup. The neutron correlation to gross gamma is expected even to improve when the cooling time increases. The assemblies are expected to have long cooling times when the final disposal of spent fuel begins. In the case of VVER assemblies it might be a good option to use ^{244}Cm neutrons vs. gross gamma as a reference curve for partial defect purposes. The other option would be that ^{244}Cm neutrons are correlated to the declared burnup with a separate verification of the burnup by gross gamma.

Using the operator declared data is inevitable in order to calculate the necessary corrections to the measured neutron and gamma data. Only the corrections for parasitic gamma emitters to the gross gamma data are independent of the declared data. These corrections are based on the measured gamma spectroscopic data only.

It is not excluded that an intelligent removal of rods could yield neutron and gamma signals, which would be consistent to an intact assembly with lower burnup. This leaves the operator a possibility to cover a possible diversion with an intelligent falsification of the burnup or other irradiation history data. For this reason it is crucial to keep a database on the irradiation histories of the spent fuel assemblies from the moment when they are inserted into the reactor. In this way it would be impossible for the operator to change later the irradiation data for dishonest purposes.

REFERENCES

1   A. Tiitta, J. Hautamäki, A. Turunen, R. Arlt, J. Arenas Carrasco, K. Esmailpour-Kazerouni, P. Schwalbach. Spent BWR Fuel Characterisation Combining a Fork Detector with Gamma Spectrometry. Report STUK-YTO-TR 175. Radiation and Nuclear Safety Authority, Helsinki, 2001.

2   R. Berndt. Verification of Spent PWR Fuel Data Using the ^{154}Eu, ^{134}Cs and ^{137}Cs Activities. Kernenergie, 1988. Vol. 31, nro 2, pp. 59–63.

3   A. Tanskanen. Assessment of the neutron and gamma sources of spent BWR fuel. Interim Report on Task JNT A 1071 FIN of the Finnish Support Programme to IAEA Safeguards. STUK-YTO-TR 170. Helsinki 2000. 17 pp + Appendices 14 pp.

4   O. J. Marttila. Säteilysuojelun käytäntö. Limes ry, Helsinki, 1989.

5   F. H. Attix, E. Tochilin. Radiation Dosimetry, Second Edition, Volume III, Sources, Fields, Measuremens and Applications. Academic Press, New York and London, 1969.

6   Per-Erik Hägg, Loviisa NPP. Private operator communication, June 2001.

RAW MEASURED DATA

Table A1.1. *Raw data of the measurements performed at three different heights z = 750 mm, z = 1250 mm, z = 1750 mm. The assemblies are identified according to the last three figures of their ID numbers in this table.*

Ass. ID	Height (mm)	Angle (deg)	non-corr N_{Cd} (cps)	error N_{Cd} (cps)	non-corr $N_{no\text{-}Cd}$ (cps)	error $N_{no\text{-}Cd}$ (cps)	non-corr G	error G	non-corr $A_{34,605}$ (cps)	error $A_{34,605}$ (%)	non-corr A_{37} (cps)	error A_{37} (%)	non-corr $A_{34,795}$ (cps)	error $A_{34,795}$ (%)	non-corr $A_{Ru/Rh}$ (cps)	error $A_{Ru/Rh}$ (%)	non-corr A_{34}/A_{37}	non-corr $A_{Ru/Rh}/A_{37}$
#621	750	45	342.26	1.85	263.93	1.62	1282.0	1.250	137.4	2.0	281.2	1.0	95.8	1.8	24.0	9.5	0.4000	0.3027
	1250	45	359.77	1.90	270.40	1.64	1282.0	1.250	136.6	1.9	286.7	1.0	98.1	1.8	23.9	9.5	0.3930	0.3011
	1750	45	308.77	1.76	235.65	1.54	1223.0	0.313	124.9	2.1	273.7	1.0	89.1	1.9	19.7	11.0	0.3758	0.2589
	750	-75	337.15	1.84	257.60	1.60	1277.0	1.250	118.0	2.3	243.4	1.2	84.8	2.2	20.5	11.6	0.4000	0.3043
	1250	-75	363.68	1.91	275.54	1.66	1302.0	1.250	132.5	2.1	269.7	1.1	96.7	1.9	26.5	9.1	0.4070	0.3585
	1750	-75	319.90	1.79	242.95	1.56	1251.0	0.313	131.9	2.0	257.6	1.1	89.4	1.9	22.2	10.4	0.4163	0.3006
#120	750	45	0.63	0.08	0.36	0.06	109.6	0.143	2.7	14.6	39.2	1.9	2.4	9.3	0.0	0.0	0.0603	0.0000
	1250	45	0.59	0.08	0.45	0.07	116.5	0.247			42.0	1.8	2.5	9.7	0.0		0.0176	0.0000
	1750	45	0.51	0.07	0.36	0.06	107.2	0.247	1.8	24.0	40.1	1.9	2.1	10.1	0.0		0.0430	0.0000
	750	-75	0.58	0.08	0.36	0.06	105.0	0.286	3.4	11.7	34.8	2.0	1.8	11.9	0.0		0.0751	0.0000
	1250	-75	0.49	0.07	0.31	0.06	114.6	0.143	3.3	12.0	38.6	1.9	2.3	9.5	0.0		0.0700	0.0000
	1750	-75	0.50	0.07	0.34	0.06	109.0	0.202	3.3	12.1	37.9	1.9	2.0	10.5	2.6	16.8	0.0689	0.2249
#764	750	45	83.13	0.91	62.07	0.79	372.5	0.313	12.0	6.7	145.6	1.0	7.4	6.0			0.0655	0.0000
	1250	45	99.96	1.00	76.49	0.87	390.0	0.313	12.6	6.7	154.1	1.0	8.1	5.4			0.0656	0.0000
	1750	45	91.12	0.95	69.61	0.83	378.7	0.313	12.8	6.4	145.8	1.0	8.9	5.3			0.0718	0.0000
	750	-75	92.20	0.96	71.01	0.84	385.0	0.313	13.1	6.3	145.5	1.0	8.9	5.3			0.0732	0.0000
	1250	-75	99.16	1.00	75.75	0.87	395.0	0.313	13.2	6.5	145.2	1.0	9.1	5.5			0.0742	0.0000
	1750	-75	81.64	0.90	62.48	0.79	375.0	0.313	13.0	6.2	141.6	1.0	8.9	5.3			0.0748	0.0000
#618	750	45	84.71	0.92	65.79	0.81	375.6	0.313	9.6	7.9	140.2	1.0	7.7	5.6			0.0582	0.0000
	1250	45	109.53	1.05	85.10	0.92	403.8	0.313	12.4	6.5	149.5	1.0	9.0	5.1			0.0686	0.0000
	1750	45	105.36	1.03	79.89	0.89	394.4	0.313	9.8	7.9	143.9	1.1	7.7	6.0			0.0575	0.0000
	750	-75	103.21	1.02	79.64	0.89	389.4	0.313	11.9	7.0	145.6	1.0	8.6	5.4			0.0675	0.0000
	1250	-75	108.94	1.04	83.75	0.92	400.6	0.313	11.6	7.1	152.5	1.0	8.5	5.7			0.0631	0.0000
	1750	-75	80.88	0.90	63.98	0.80	367.5	0.313	12.1	6.6	139.4	1.1	8.5	5.4			0.0712	0.0000
#018	750	45	137.53	1.17	103.97	1.02	816.3	0.313	87.4	2.4	193.9	1.1	58.5	2.1	19.3	8.9	0.3653	0.3446
	1250	45	168.87	1.30	128.04	1.13	868.7	0.313	87.0	2.3	203.8	1.1	60.8	2.1	19.6	8.8	0.3497	0.3416
	1750	45	165.65	1.29	127.82	1.13	862.5	0.313	84.0	2.4	196.5	1.1	59.9	2.2	22.8	7.6	0.3520	0.4172
	750	-75	166.46	1.29	128.13	1.13	872.5	0.313	85.9	2.3	202.2	1.1	62.6	2.1	22.8	7.7	0.3518	0.4110
	1250	-75	167.87	1.30	127.50	1.13	875.6	0.313	87.3	2.6	199.6	1.1	63.3	2.1	22.5	7.7	0.3617	0.4096
	1750	-75	127.42	1.13	99.96	1.00	808.7	0.313	78.2	2.2	191.7	1.1	52.9	2.2	19.5	8.5	0.3315	0.3544
#705	750	45	92.69	0.96	70.32	0.84	876.2	0.313	83.8	2.3	206.0	1.1	55.8	2.2	17.0	10.3	0.3293	0.2849
	1250	45	99.61	1.00	74.53	0.86	891.3	0.313	96.6	2.3	207.0	1.1	57.4	2.3	16.7	10.1	0.3678	0.2619
	1750	45	96.18	0.98	70.67	0.84	866.9	0.313	79.4	2.4	203.2	1.1	58.8	2.1	18.0	9.6	0.3249	0.3262
	1750	-75	94.28	0.97	71.18	0.84	861.9	0.313	77.0	2.4	195.4	1.1	55.5	2.1	18.0	9.2	0.3254	0.3335
	1250	-75	99.09	1.00	74.60	0.86	885.6	0.313	81.6	2.2	201.0	1.1	58.1	2.2	19.8	9.0	0.3342	0.3539
	750	-75	89.32	0.95	68.41	0.83	865.0	0.313	73.9	2.6	184.8	1.2	48.5	2.7	15.2	11.1	0.3225	0.2816

ANNEX 1 RAW MEASURED DATA

Table A1.I. (continues)

Ass. ID	Height (mm)	Angle (deg)	non-corr N_{Cd} (cps)	error N_{Cd} (cps)	non-corr N_{no-Cd} (cps)	error N_{no-Cd} (cps)	non-corr G	error G	non-corr $A_{34,605}$ (cps)	error $A_{34,605}$ (%)	non-corr A_{37} (cps)	error A_{37} (%)	non-corr $A_{34,795}$ (cps)	error $A_{34,795}$ (%)	non-corr $A_{Ru/Rh}$ (cps)	error $A_{Ru/Rh}$ (%)	non-corr A_{34}/A_{37}	non-corr $A_{Ru/Rh}/A_3$
#046	750	45	171.88	1.31	132.77	1.15	573.8	0.313	35.4	3.5	184.7	1.0	22.2	3.5			0.1529	0.0000
	1250	45	209.77	1.45	161.42	1.27	605.0	0.313	37.1	3.4	200.0	1.0	25.8	3.0			0.1518	0.0000
	1750	45	205.25	1.43	157.26	1.25	596.9	0.313	33.3	3.9	199.3	1.0	24.8	3.1			0.1391	0.0000
	1750	−75	202.53	1.42	157.38	1.25	588.1	0.313	32.9	3.6	172.5	1.0	21.8	3.3			0.1542	0.0000
	1250	−75	207.74	1.44	162.09	1.27	588.8	0.313	32.6	3.6	177.5	1.0	22.5	3.3			0.1500	0.0000
	750	−75	164.85	1.28	129.93	1.14	549.4	0.313	29.7	3.8	166.7	1.0	20.5	3.4			0.1455	0.0000
#319	750	45	245.11	1.57	187.28	1.37	573.1	0.313	32.6	3.6	192.2	1.0	21.8	3.5	0.0		0.1374	0.0000
	1250	45	350.24	1.87	265.07	1.63	640.0	0.313	37.1	3.4	209.9	0.9	23.4	3.5	0.0		0.1412	0.0000
	1750	45	336.38	1.83	257.61	1.61	626.9	0.313	36.5	3.4	201.9	0.9	25.3	3.1	0.0		0.1478	0.0000
	1750	−75	339.36	1.84	257.70	1.61	648.8	0.313	39.9	3.5	230.5	0.9	26.8	3.2	0.0		0.1404	0.0000
	1250	−75	345.47	1.86	264.30	1.63	656.9	0.313	39.1	3.7	236.0	0.9	29.6	3.0	0.0		0.1386	0.0000
	750	−75	236.48	1.54	179.36	1.34	582.5	0.313	38.1	3.4	214.0	0.9	24.8	3.3	2.9	40.6	0.1433	0.0462
#628	750	45	158.25	1.26	116.99	1.08	492.5	0.313	12.6	7.2	193.3	0.9	9.1	5.6			0.0538	0.0000
	1250	45	170.24	1.30	126.68	1.13	498.8	0.313	14.0	6.6	188.7	0.9	9.0	5.4			0.0595	0.0000
	1750	45	144.58	1.20	110.59	1.05	476.9	0.313	12.7	6.9	183.3	0.9	8.7	5.7			0.0565	0.0000
	1750	−75	149.43	1.22	110.70	1.05	500.6	0.313	17.0	6.1	234.9	0.8	12.3	4.7			0.0598	0.0000
	1250	−75	169.81	1.30	126.04	1.12	523.8	0.313	17.3	6.0	238.7	0.9	12.8	4.8			0.0603	0.0000
	750	−75	154.01	1.24	115.50	1.07	514.4	0.313	15.7	6.8	225.7	0.9	10.1	6.6			0.0558	0.0000
#037	750	45	261.65	1.62	198.97	1.41	591.3	0.313	25.8	4.5	174.6	1.0	18.9	3.7			0.1225	0.0000
	1250	45	318.93	1.79	246.65	1.57	630.0	0.313	32.0	3.8	195.2	1.0	22.2	3.4			0.1340	0.0000
	1750	45	306.25	1.75	237.64	1.54	622.5	0.313	34.4	3.6	196.3	1.0	23.5	3.2			0.1427	0.0000
	1750	−75	309.64	1.76	239.26	1.55	632.5	0.313	41.7	3.3	222.5	0.9	25.3	3.2			0.1484	0.0000
	1250	−75	320.66	1.79	243.81	1.56	639.4	0.313	40.2	3.3	223.7	0.9	26.3	3.1			0.1448	0.0000
	750	−75	251.32	1.59	192.32	1.39	591.9	0.313	34.4	3.6	208.5	0.9	22.2	3.5			0.1325	0.0000
#932	750	45	235.95	1.54	177.07	1.33	809.4	0.313	65.3	2.5	268.2	0.9	44.6	2.5	0.0		0.1983	0.0000
	1250	45	256.63	1.60	191.03	1.38	824.4	0.313	65.7	2.7	268.8	0.9	44.5	2.5	0.0		0.1987	0.0000
	1750	45	222.55	1.49	165.98	1.29	784.4	0.313	62.8	2.6	253.5	0.9	42.6	2.5	4.0	36.8	0.2014	0.0551
	1750	−75	213.91	1.46	166.80	1.29	764.4	0.313	51.4	2.9	230.1	0.9	33.7	2.8	0.0		0.1801	0.0000
	1250	−75	251.26	1.59	192.13	1.39	808.1	0.313	54.8	2.8	236.6	0.9	35.8	2.7	0.0		0.1866	0.0000
	750	−75	228.61	1.51	174.14	1.32	790.6	0.313	46.5	3.2	217.0	1.0	32.5	3.3	0.0		0.1755	0.0000
#974	750	45	314.49	1.77	242.07	1.56	1038.0	0.313	88.9	2.3	244.6	1.0	59.3	2.2	0.0		0.2943	0.0000
	1250	45	372.10	1.93	284.96	1.69	1087.0	0.313	89.7	2.4	253.6	1.0	61.7	2.2	15.8	11.8	0.2886	0.2192
	1750	45	351.37	1.87	270.59	1.64	1064.0	0.313	88.6	2.2	250.3	1.0	61.6	2.2	12.7	14.3	0.2896	0.1797
	1750	−75	355.30	1.88	271.22	1.65	1088.0	0.313	103.9	2.3	274.2	1.0	69.9	2.0	13.4	15.0	0.3075	0.1697
	1250	−75	377.99	1.94	288.75	1.70	1111.0	0.313	104.6	2.2	288.3	0.9	71.5	2.1	0.0		0.2956	0.0000
	750	−75	309.63	1.76	233.29	1.53	1041.0	0.313	101.5	2.2	267.2	1.0	65.7	2.1	0.0		0.3054	0.0000

RAW MEASURED DATA

Table A1.1. *(continues).*

Ass. ID	Height (mm)	Angle (deg)	non-corr N_{Cd} (cps)	error N_{Cd} (cps)	non-corr $N_{no\text{-}Cd}$ (cps)	error $N_{no\text{-}Cd}$ (cps)	non-corr G	error G	non-corr $A_{34,605}$ (cps)	error $A_{34,605}$ (%)	non-corr A_{37} (cps)	error A_{37} (%)	non-corr $A_{34,795}$ (cps)	error $A_{34,795}$ (%)	non-corr $A_{Ru/Rh}$ (cps)	error $A_{Ru/Rh}$ (%)	non-corr A_{34}/A_{37}	non-corr $A_{Ru/Rh}/A_3$
#402	750	45	417.12	2.04	317.93	1.78	2243.0	1.250	294.9	1.7	319.3	1.3	207.6	1.7	94.5	4.8	0.7580	1.0559
	1250	45	495.64	2.23	379.87	1.95	2376.0	1.250	325.5	1.7	324.2	1.4	213.2	1.7	109.1	4.7	0.8094	1.1508
	1750	45	474.55	2.18	360.53	1.90	2329.0	1.250	313.6	1.7	329.6	1.3	215.4	1.6	110.3	4.3	0.7760	1.1763
	1750	-75	468.64	2.16	363.11	1.91	2311.0	1.250	284.1	1.7	308.8	1.3	203.2	1.7	96.4	4.6	0.7581	1.1247
	1250	-75	493.38	2.22	377.91	1.94	2344.0	1.250	281.8	1.7	317.5	1.4	205.1	1.6	94.7	4.7	0.7347	1.0864
	750	-75	406.83	2.02	310.43	1.76	2170.0	1.250	264.5	1.8	291.2	1.4	177.5	1.6	91.8	4.4	0.7366	1.0931
#903	750	45	457.50	2.14	348.71	1.87	1034.0	0.313	80.9	2.5	292.5	0.9	55.2	2.4	0.0		0.2252	0.0000
	1250	45	492.91	2.22	372.95	1.93	1052.0	0.313	85.1	2.4	302.0	0.9	58.2	2.3	0.0		0.2296	0.0000
	1750	45	447.30	2.11	340.79	1.85	1014.0	0.313	80.9	2.4	284.8	0.9	55.7	2.2	0.0		0.2318	0.0000
	1750	-75	443.81	2.11	334.76	1.83	998.1	0.313	80.7	2.5	280.1	0.9	53.3	2.4	7.8	23.4	0.2327	0.0957
	1250	-75	492.48	2.22	374.54	1.94	1047.0	0.313	89.6	2.3	295.4	0.9	61.2	2.2	0.0		0.2471	0.0000
	750	-75	452.20	2.13	343.77	1.85	1026.0	0.313	83.4	2.4	285.8	0.9	56.8	2.3	7.7	22.6	0.2375	0.0942
#637	750	45	572.29	2.39	434.51	2.08	785.0	0.313	32.6	4.3	297.0	0.8	23.9	3.5			0.0910	0.0000
	1250	45	615.26	2.48	469.51	2.17	800.6	0.313	35.7	4.1	305.6	0.8	24.1	3.5			0.0949	0.0000
	1750	45	570.06	2.39	434.35	2.08	778.1	0.313	34.7	4.2	293.5	0.8	25.8	3.4			0.0984	0.0000
	1750	-75	568.11	2.38	433.80	2.08	776.9	0.313	32.7	4.2	288.0	0.8	21.8	3.8			0.0919	0.0000
	1250	-75	619.19	2.49	471.18	2.17	801.2	0.313	31.2	4.6	299.9	0.8	22.9	3.6			0.0863	0.0000
	750	-75	563.64	2.37	432.08	2.08	781.9	0.313	31.2	4.4	282.2	0.8	21.8	3.9			0.0906	0.0000
#432	750	45	288.51	1.70	218.23	1.48	975.0	0.313	95.2	2.3	252.3	1.0	66.5	2.1	18.4	10.3	0.3091	0.2590
	1250	45	304.56	1.75	229.70	1.52	989.4	0.313	97.8	2.1	265.3	1.0	67.7	2.0	20.3	9.6	0.3013	0.2702
	1750	45	261.78	1.62	199.86	1.41	939.4	0.313	90.3	2.3	243.3	1.0	63.7	2.1	17.3	10.7	0.3048	0.2540
	1750	-75	261.73	1.62	200.36	1.42	953.1	0.313	88.7	2.2	241.1	1.0	60.4	2.2	19.3	9.5	0.2994	0.2799
	1250	-75	300.48	1.73	229.18	1.51	1005.0	0.313	88.8	2.5	255.6	1.0	63.2	2.2	15.3	12.4	0.2859	0.2150
	750	-75	281.38	1.68	212.21	1.46	989.4	0.313	87.3	2.3	240.4	1.0	56.7	2.4	16.9	12.0	0.2922	0.2393
#532	750	45	266.89	1.63	204.83	1.43	862.5	0.313	63.8	2.6	243.0	0.9	42.7	2.5			0.2128	0.0000
	1250	45	288.67	1.70	219.94	1.48	879.4	0.313	65.7	2.6	250.3	0.9	44.7	2.5			0.2136	0.0000
	1750	45	263.81	1.62	198.29	1.41	846.9	0.313	62.2	2.7	237.7	0.9	43.4	2.4			0.2143	0.0000
	1750	-75	264.87	1.63	200.08	1.41	863.7	0.313	72.5	2.5	265.1	0.9	50.2	2.3			0.2235	0.0000
	1250	-75	288.19	1.70	219.26	1.48	893.7	0.313	78.2	2.4	270.9	0.9	50.1	2.3			0.2315	0.0000
	750	-75	265.66	1.63	199.12	1.41	870.0	0.313	69.1	2.7	253.3	0.9	50.8	2.5			0.2264	0.0000
#649	750	45	203.41	1.43	154.10	1.24	766.9	0.313	50.3	2.9	221.9	1.0	33.5	2.8			0.1835	0.0000
	1250	45	219.14	1.48	170.20	1.30	781.3	0.313	50.6	3.0	227.5	0.9	34.5	2.8			0.1811	0.0000
	1750	45	196.28	1.40	150.95	1.23	750.6	0.313	47.8	3.0	213.1	1.0	30.3	2.9			0.1794	0.0000
	1750	-75	200.25	1.42	150.78	1.23	763.1	0.313	55.2	2.9	237.7	0.9	36.7	2.7			0.1879	0.0000
	1250	-75	223.01	1.49	169.15	1.30	793.1	0.313	55.0	2.8	240.0	0.9	39.9	2.6			0.1895	0.0000
	750	-75	203.74	1.43	153.86	1.24	776.3	0.313	52.4	2.9	232.5	0.9	37.5	2.7			0.1857	0.0000

ANNEX 1 RAW MEASURED DATA

Table A1.II. Raw data of the axial scanning measurement of the assembly #13640621 (angle = 45 degrees).

Height (mm)	non-corr N_{Cd} (cps)	error N_{Cd} (cps)	non-corr N_{no-Cd} (cps)	error N_{no-Cd} (cps)	non-corr G	error G	non-corr $A_{34,605}$ (cps)	error $A_{34,605}$ (%)	non-corr A_{37} (cps)	error A_{37} (%)	non-corr $A_{34,795}$ (cps)	error $A_{34,795}$ (%)	non-corr $A_{Ru/Rh}$ (cps)	error $A_{Ru/Rh}$ (%)	non-corr A_{34}/A_{37}	non-corr A_{Ru-106}/A_{37}
2500	3.96	0.20	3.27	0.18	209.0	0.247										
2250	74.98	0.87	57.88	0.76	720.0	0.313	64.2	2.6	182.3	1.1	45.7	2.3			0.2898	
2000	221.69	1.49	169.38	1.30	1087.0	0.313	110.9	2.1	248.9	1.0	78.5	1.9	19.3	10.1	0.3662	0.2776
1750	308.77	1.76	235.65	1.54	1223.0	0.313	124.9	2.1	273.7	1.0	89.1	1.9	19.7	11.0	0.3758	0.2589
1500	345.75	1.86	263.35	1.62	1265.0	1.250	130.3	2.0	280.0	1.0	94.6	1.9	26.8	9.2	0.3850	0.3481
1250	359.77	1.90	270.40	1.64	1282.0	1.250	136.6	1.9	286.7	1.0	98.1	1.8	23.9	9.5	0.3930	0.3011
1000	362.24	1.90	270.12	1.64	1287.0	1.250	131.5	2.1	287.8	1.0	97.0	1.8	23.0	10.3	0.3796	0.2936
750	342.26	1.85	263.93	1.62	1282.0	1.250	137.4	2.0	281.2	1.0	95.8	1.8	24.0	9.5	0.4000	0.3027
500	269.07	1.64	205.66	1.43	1174.0	0.313	117.6	2.1	263.3	1.1	86.7	1.9	23.1	9.5	0.3710	0.3222
250	109.23	1.05	83.22	0.91	843.1	0.313	76.8	2.5	211.4	1.0	55.6	2.3	14.9	11.5	0.3003	0.2559
0	4.61	0.21	4.20	0.20	366.2	0.313										

PYVO CALCULATIONS

Table A2.I. ^{244}Cm neutron source (n/s/t) dependence on enrichment and burnup at discharge calculated with PYVO.

Enrich-ment (w-%)	Burnup (MWd/kgU)						
	15	20	25	30	35	40	45
1.6	3.871108E+07	1.469576E+08	3.886450E+08	8.188603E+08	1.476161E+09	2.376441E+09	3.513879E+09
1.8	2.969473E+07	1.165135E+08	3.172445E+08	6.862638E+08	1.266768E+09	2.082576E+09	3.136151E+09
2	2.310569E+07	9.319349E+07	2.601563E+08	5.759318E+08	1.086139E+09	1.820991E+09	2.790877E+09
2.2	1.823046E+07	7.525539E+07	2.145722E+08	4.846385E+08	9.315663E+08	1.590140E+09	2.477910E+09
2.4	1.457650E+07	6.136184E+07	1.781210E+08	4.092905E+08	8.000576E+08	1.388025E+09	2.196561E+09
2.6	1.179761E+07	5.049999E+07	1.488598E+08	3.471542E+08	6.886161E+08	1.212127E+09	1.945447E+09
2.8	9.657542E+06	4.193533E+07	1.252618E+08	2.958834E+08	5.944168E+08	1.059756E+09	1.722726E+09
3	7.990111E+06	3.512430E+07	1.061192E+08	2.534511E+08	5.148291E+08	9.282266E+08	1.526212E+09
3.2	6.673463E+06	2.965562E+07	9.049281E+07	2.182186E+08	4.475399E+08	8.148802E+08	1.353454E+09
3.4	5.622881E+06	2.522621E+07	7.765253E+07	1.888402E+08	3.905649E+08	7.172985E+08	1.202091E+09
3.6	4.772952E+06	2.159713E+07	6.700237E+07	1.641656E+08	3.420871E+08	6.330921E+08	1.069455E+09
3.8	4.084395E+06	1.862431E+07	5.817895E+07	1.434793E+08	3.009258E+08	5.606297E+08	9.536164E+08
4	3.505146E+06	1.610805E+07	5.066914E+07	1.257762E+08	2.654958E+08	4.977959E+08	8.522399E+08
4.2	3.017471E+06	1.397589E+07	4.426677E+07	1.105917E+08	2.349185E+08	4.431919E+08	7.633973E+08

Table A2.II. ^{137}Cs gamma source and ^{244}Cm neutron source dependence on off-reactor cycles at discharge calculated with PYVO.

B (MWd/kg)	IE (%)	j-o-k	A_{37} (Ci/t)	^{244}Cm neutron intensity (n/s/t)
34.192	3.6	0-0-3	1.093600E+05	3.06231400E+08
34.192	3.6	1-5-2	1.053080E+05	3.05141100E+08
34.192	3.6	2-5-1	1.011410E+05	3.03944200E+08
34.192	3.6	0-0-5	1.069866E+05	3.02738000E+08
34.192	3.6	1-5-4	1.046650E+05	3.01703900E+08
34.192	3.6	2-5-3	1.022780E+05	3.01549600E+08
34.192	3.6	3-5-2	9.983385E+04	3.01840400E+08
34.192	3.6	4-5-1	9.732805E+04	2.90388600E+08
25.000	3.6	0-0-5	7.810359E+04	6.60812200E+07
25.000	3.6	3-5-2	7.288152E+04	6.61157800E+07
34.192	2.4	0-0-5	1.073028E+05	7.14190600E+08
34.192	2.4	3-5-2	1.001301E+05	7.10730100E+08
34.192	3.6	1-4-4	1.051065E+05	3.01834500E+08
34.192	3.6	4-4-1	9.934335E+04	2.92896800E+08
34.192	3.6	1-3-4	1.056103E+05	3.02115600E+08
34.192	3.6	4-3-1	1.012619E+05	2.95268600E+08
34.192	3.6	4-2-1	1.031090E+05	2.97611100E+08
34.192	3.6	2-2-1	1.060627E+05	3.05256900E+08
34.192	3.6	1-2-2	1.077348E+05	3.05786900E+08
34.192	3.6	1-1-4	1.064332E+05	3.02427100E+08
34.192	3.6	4-1-1	1.048667E+05	2.99911900E+08

ANNEX 2

<div align="right">PYVO CALCULATIONS</div>

Table A2.III. *The share of* ^{244}*Cm neutrons out of the total neutron counts at measurement data calculated with PYVO.*

Ass. ID	^{244}Cm/total neutron source (%)
13640621	96.39557
13648120	3.76544
22414764	92.591
22424618	93.77051
22432018	95.89286
13642705	93.21236
22432046	96.08296
22421319	96.16226
13617628	93.62011
22432037	96.71669
13632932	95.60254
23632974	96.75889
23644402	96.24539
13632903	96.96869
13624637	96.77266
13624432	94.34455
13624532	96.24356
13632649	95.63544